scientific reports



OPEN

Sustainable hybrid systems for electric vehicle charging infrastructures in regional applications

Aykut Fatih Güven^{1⊠}, Nilya Ateş², Saud Alotaibi³, Thabet Alzahrani³, Amare Merfo Amsal^{4⊠} & Salah K. Elsayed⁵

Increasing greenhouse gas (GHG) emissions and environmental issues have heightened the demand for renewable energy sources (RES) and prompted a swift transition to electric vehicles (EVs) in the transportation sector. This shift underscores the need to address the challenges of electricity supply and continuity for electric vehicle charging stations (EVCS). This study aims to determine the most suitable hybrid systems to ensure the electricity supply to EVCSs in the Çukurova region of Adana, Turkey. Six different scenarios involving components such as photovoltaic (PV) panel, wind turbine (WT), biomass generators (BG), electrolyzer (Elz), hydrogen tank (HT), fuel cell (FC), batteries (Bat), inverter (Inv), and the grid were analyzed using HOMER Pro microgrid analysis tool version 3.14.2 software. The optimization results indicated that the most feasible system was Scenario 4, comprising the PV, BG, Elz, HT, FC, Inv, and grid components. This scenario's total net present cost (NPC) was \$611,283.50, with a levelized cost of energy (LCOE) of \$0.0215. The annual energy production and consumption were 1,507,169 kWh and 1,420,714 kWh, respectively. The fact that the energy generated from exceeds the energy sourced from the grid reduces the payback period of the system. These findings highlight the economic and sustainable potential of renewable hybrid systems for enhancing the performance of EVCS in solar-rich regions.

Keywords Energy cost efficiency, Renewable energy integration, Electric vehicle charging stations, Hybrid systems, Optimization, Energy sustainability

Abbreviations

Alternating current ACC Annual capital costs BTS Battery storage **BEV** Battery electric vehicle BG Biomass generator CF Capacity factor CO Carbon monoxide CO. Carbon dioxide COE Cost of energy DC Direct current DG Diesel generator Elz Electrolyzer EV Electric vehicle

EVCS Electric vehicle charging station

n Generator GHG Greenhouse gas

¹Department of Electrical and Electronics Engineering, Yalova University, Yalova, Turkey. ²Ekosmart Energy, Kocaeli, Turkey. ³Electrical Engineering Department, College of Engineering, Shaqra University, Al Duwadimi, 11911 Riyadh, Saudi Arabia. ⁴Department of Mechanical Engineering, Faculty of Technology, Debre Markos University, P. O. Box 269, Debre Markos, Ethiopia. ⁵Department of Electrical Engineering, College of Engineering, Taif University, Taif 21944, Saudi Arabia. [⊠]email: afatih.guven@yalova.edu.tr; amare_merfo@dmu.edu.et

Hybrid renewable energy systems **HRES**

Hybrid electric vehicles HEV

HOMER Pro hybrid optimization of multiple energy resources

HT Hydrogen tank Inv Inverter

LCOE Levelized cost of energy NOx Nitrogen oxides NPC Net present cost

PHEV Plug-ın hybrid electric vehicle

PM Particulate matter PVPhotovoltaic **RES** Wind energy systems WT Wind turbine SO₂ Sulfur dioxide

REŠs Renewable energy sources

FC Fuel cell

UHC Unburned hydrocarbons

List of symbols

Swept area of turbine blades A_{RT} BE_T Total biomass consumption $B_{rated}\left(t\right)$ Hourly biomass consumption rate

 $BG_{p}\left(t\right)$ Generator output power Capital recovery factor CRF C_p Power coefficient $C_{ann,tot}$ Total annual cost C_{boiler} Boiler marginal cost $E_{\substack{served \ RT}}$ Total electrical load served Initial costs of wind turbines

C_{ACC} RT C_{rep} Replacement cost E_{ac}^{G} EG(t)Energy output

Electricity produced by the battery at time t

Direct current energy produced EDCAlternating current energy produced EAC

Electricity generated E_G

Energy required to drive an electric vehicle Ek

Electricity demand

 $E_L \\ EBat(t)$ Energy level of the battery at time t EBat(t-1)Energy level of the battery at time t-1 $F_{BG}(t)$ Hourly average fuel consumption Marginal fuel consumption F_m

Fuel consumption without a load factor F_0 FC_P Electricity generated in fuel cells GP_{rat} Power rating of the generator GWPGlobal warming potential

Number of generators used in the experiment G_N

Total thermal load served H_{served} Mass of hydrogen stored in tank HT_m

Higher heating value of stored hydrogen gas HHV_H

Kilometers driven by electric vehicles Kd LHV_{sy}

Lower heating temperature of the synthesis gas Lower heating value of the raw material LHV_{B}

Lifetime of the wind turbine $N_{wind.1}$ PV_p Power generated by PVs PV_N Number of PV units PV_{η}^{N} PV_{p}^{rat} Efficiency of the PV module

PV-rated power $P_0 P_{Ht/FC}(t)$ Actual power output

Power supplied from the hydrogen tank to the fuel cell

Power generated from renewable sources

 $P_{ren} P_{ren/ELE}$ Electricity supplied to the electrolyzer from renewable sources

 P_{RT_rated} Power rating of the wind turbine

 R_{proj} Project lifetime

Remaining lifecycle of wind turbines $\underset{SOC}{R_{return}}$

State of charge

SOCmax Maximum state of charge

 $SR_{int}(t)$ Intensity of solar radiation at time t Cell temperature of the solar panel T_C

Ambient temperature T_A

 T_r Reference temperature of the solar panel

 T_{nor} Cell temperature under normal operating conditions

QbatchBattery capacity W_{η} Wiring efficiency

 δ_T Maximum temperature coefficient of the solar panel module

 v_1 Wind speed measured at the anemometer's height

 v_2 Wind speed recorded at a specified height of the wind turbine hub

 h_1 Height at which the anemometer is positioned h_2 Designated height of the wind turbine hub

 v_{cut-in} Minimum wind speed required for the turbine to generate electricity

 $v_{cut-off}$ Wind speed threshold at which the turbine stops operation for safety reasons

 ρ Air density

σ Self-discharge rate of the battery on an hourly basis

 η_{conv} Converter efficiency

 η_{CC} Efficiency of charge controller η_{rbat} Round-trip efficiency of the battery

 $\begin{array}{ll} \eta_{inv} & \text{Efficiency of the inverter} \\ \eta_{HT} & \text{Efficiency of hydrogen tank} \\ \eta_{FC} & \text{Efficiency of fuel cell} \\ \eta_{sy} & \text{Efficiency of gas synthesis} \\ m_{sy} & \text{Mass flow of the synthetic gas} \\ \Delta t & \text{Duration of simulation} \end{array}$

Motivation

Energy remains a cornerstone in today's interconnected world, significantly driving nations' growth and development. The continuous increase in global energy demand underscores its role not only as a necessity but also as a fundamental contributor to both social and economic progress. The rising demand for energy has made it crucial to adopt sustainable energy management strategies across diverse regions and timeframes¹. Nonetheless, the excessive and often unmonitored exploitation of energy resources has led to their rapid depletion, raising concerns about long-term sustainability. Consequently, there has been a strong shift toward exploring alternative energy solutions, with renewable energy sources (RESs), including solar and wind, standing out due to their environmentally friendly and inexhaustible nature².

The incorporation of RESs into electrical grids has proven to be highly versatile, with applications ranging from residential settings to industrial sectors and electric vehicle charging infrastructure³. This adaptability has led to increased interest in hybrid renewable energy systems (HRESs) and microgrids, encouraging researchers to assess these systems based on energy efficiency and sustainability. Additionally, the growing adoption of electric vehicles (EVs) has further shifted attention toward optimizing their performance and conducting technical and economic analyses from multiple perspectives⁴. Integrating EVs into power grid operations presents various advantages, such as reduced generation costs, improved voltage stability, and decreased power losses and emissions⁵.

With continuous technological advancements, the imperative to modernize conventional electrical grids to accommodate both EVs and RESs has become increasingly apparent⁶. Nonetheless, the variable energy demands of EVs, along with the integration of renewable energy sources, present significant challenges in terms of grid management and system design⁷. Thus, accurate modeling and optimization of grid-integrated, renewable energy-driven EV charging systems are essential to achieve maximum technical performance and economic efficiency. This section addresses the growing global energy demand, underscores the critical role of renewable energy in meeting these needs, and explores the challenges and opportunities presented by the integration of EVs into energy infrastructure. By doing so, the study establishes the context and identifies existing research gaps in the literature.

Literature review

EVs represent a significant leap forward in the transportation sector due to their zero-emissions nature. With the global EV fleet currently numbering around three million and projections suggesting an increase to 100 million by 2030, the need for extensive and efficient charging infrastructure is becoming increasingly urgent. However, ensuring the sustainability of EVs is highly dependent on the source of electricity used. Fossil fuel-based electricity generation shifts pollution from vehicle emissions to power plants. Therefore, transitioning to renewable and sustainable energy sources is essential to reduce greenhouse gas emissions and promote environmental sustainability⁸.

Among the various renewable energy technologies available, solar photovoltaic (PV) systems have proven to be one of the most effective solutions for EV charging infrastructure. PV technology is particularly advantageous due to its applicability in both urban and rural areas. Solar PV systems significantly reduce greenhouse gas (GHG) emissions, lower energy costs, and encourage the widespread adoption of solar energy. These systems can be deployed either as grid-tied or standalone units, supporting a variety of sectors, including residential, healthcare, and commercial applications, thus accelerating the integration of EVs⁹.

In recent years, Turkey has made notable strides in expanding its energy portfolio by increasing its reliance on renewable energy sources. According to data from TEİAŞ, Turkey's total installed capacity in 2012 was 57,059.4 megawatt (MW), with the majority coming from thermal power (61.4%). Hydroelectric power contributed 34.4%, followed by wind energy at 4.0% and geothermal at 0.3%. Notably, solar energy was not yet a part of the mix at that time. By 2022, the installed capacity had increased to 103,809.3 MW; with a significant

shift in the energy mix: thermal power decreased to 47.9%, hydroelectric power to 30.4%, geothermal power to 1.6%, wind power to 11.0%, and solar power to 9.1%. This trend continued into 2023 and 2024, with solar energy representing 12.2% of the total installed capacity of 108,552.9 MW. These figures demonstrate Turkey's commitment to diversifying its energy sources, reducing its dependence on fossil fuels, and enhancing energy security and sustainability 10 .

This shift toward renewable energy is reflected in Turkey's expanding EV market and the accompanying need for charging infrastructure. Projections indicate a significant increase in both the number of EVs and the number of charging stations by 2035. In 2025, the EV population is expected to range from 202,030 to 361,893, ranging from 776,362 to 1,679,600 by 2030, and reaching 4,214,273 by 2035. As a result, the number of charging stations is also expected to rise substantially. Recent analyses indicate considerable growth in DC fast charging stations, underscoring the importance of developing robust infrastructure to support the increasing adoption of EVs in Turkey¹¹.

While the use of solar energy in EV charging is becoming more widespread, there are several challenges associated with relying solely on solar PVs. One major limitation is the dependency on weather and atmospheric conditions, which leads to fluctuations in energy production, with peak generation occurring during the day and zero generation at night. Additionally, without proper regulation, overproduction during periods of high solar irradiance can occur. On the other hand, grid-connected systems offer a solution by sending surplus electricity back to the grid, thereby maximizing revenue opportunities. The findings in the literature highlight an increasing emphasis on the development of advanced electric vehicle (EV) charging infrastructure and the optimization of EV charging demand management. This underscores the critical need for innovative approaches and solutions to address the challenges that emerge in this rapidly evolving sector.

Recent research has emphasized the techno-economic impacts of HRES for Electric Vehicle Charging Station (EVCS). For example¹², explores a renewable energy-based hybrid energy storage system in Malaysia, incorporating PV, wind turbine (WT), lithium-ion batteries, and hydrogen technologies to address challenges like grid instability and high electricity demand. This work demonstrates the adaptability of hybrid energy systems across various meteorological conditions, emphasizing their potential to promote economic and environmental sustainability. Similarly¹³, highlights a two-level charging scheduling framework that reduces grid peak demand and flattens aggregate load through advanced optimization techniques like reinforcement learning, offering practical solutions for efficient EVCS operation.

In regions vulnerable to climate change, renewable energy integration plays a pivotal role. In¹⁴, an off-grid PV-wind-hydrogen storage-based EVCS system in Pakistan illustrates how geographical and climate factors influence energy generation, system size, and economic parameters. The study underscores the importance of optimal sizing and location-specific customization to achieve cost-effective renewable integration. Further¹⁵, investigates reliability challenges in areas with frequent grid outages, finding that PV-battery-hydrogen systems significantly enhance system reliability while emphasizing the need for advancements in hydrogen storage to reduce costs.

The study in 16 investigates the interplay between demand response strategies and energy storage planning by incorporating residential-scale EVCS infrastructure. By implementing multi-objective optimization models, this work demonstrates the potential for increased revenue and reduced carbon emissions, reinforcing the importance of comprehensive demand-side management 17. introduces mobile charging stations (MCS) as a novel solution for user convenience and grid efficiency, addressing challenges like high operational costs and charging congestion through advanced clustering and scheduling algorithms.

In¹⁸, a two-stage optimization strategy is used to plan EVCS and distributed generators (DGs) within coupled transportation and distribution networks, improving cost-effectiveness and operational efficiency. This study highlights the incremental benefits for EVCS and grid operators, demonstrating the potential for integrated planning frameworks. Similarly¹⁹, evaluates PV-hydrogen and PV-hydrogen-battery configurations in Pakistan, showing that hybrid systems combining hydrogen and battery storage (BTS) offer superior financial performance and energy reliability compared to standalone systems.

The integration of hybrid energy storage systems, including hydrogen and batteries, into renewable microgrids is further explored in²⁰. Using advanced optimization algorithms like Levy Flight, this study achieves substantial cost reductions and enhanced system reliability, contributing to the broader adoption of HRES in microgrid applications. In line with this²¹, investigates optimal fast-charging station placement using distributed PV generation to reduce power losses and improve network reliability, emphasizing the critical role of spatial optimization in EVCS deployment.

Real-world applications, as illustrated in²², assess the sustainability of EVCS locations through multicriteria decision-making frameworks, highlighting economic and technical considerations as key factors in site selection. Hybrid algorithms proposed in²³ enable the integration of EVCS into distribution networks, focusing on voltage stability, power loss, and sustainability goals²⁴. reviews strategies for capacity allocation and control in PV-integrated EVCS systems, highlighting solutions to mitigate uncertainties in solar output and EV charging demand, ensuring grid stability and economic efficiency.

In Pakistan, a system integrating PV panels, BTS, and EVs achieved a 45% reduction in energy costs through an optimal energy management system (EMS), with EVs further contributed to cost savings²⁵. A similar approach using PV and biogas (BG) in an unspecified location led to a 74.67% reduction in the energy costs of EV charging stations (EVCS)²⁶. In Saudi Arabia, a PV- WT-battery system was found to be economically viable²⁷, whereas in Northern Alberta, the integration of fuel cells (FC) into a PV-WT-based battery configuration was identified as the optimal solution²⁸. Studies using Python-based models have highlighted the importance of combining technical, economic, and environmental evaluations for hybrid systems²⁹.

In Morocco, the Dakhla region has been identified as the most suitable region for hybrid systems using PV and wind energy³⁰. Denmark's Aalborg and Hirtshals regions show high renewable energy potential with PV, WT,

biomass, and BTS³¹. Ethiopia's research revealed that a ZnBr battery is most appropriate for hybrid systems³². In the United States, PV-supported microgrids in Florida that integrate EVs reduced carbon emissions by 44% and system costs by 9.5%³³. A study comparing the Netherlands and India demonstrated significant economic and environmental benefits from optimized EVCS setups incorporating PVs, WTs, BTS, and EVs³⁴. In India, systems utilizing solar PV and BTS storage were found to be economically viable and optimized for selling surplus energy back to the grid³⁵.

In Saudi Arabia, an integrated hybrid system using PV, WT, BTS, and EVs annually produced 191,221 kWh, proving to be both economically and environmentally sustainable²⁶. Similarly, in Arizona, USA, an optimized hybrid system reduced energy costs to \$0.0420/kWh, with a total net present cost (NPC) of \$1,600,623³⁶. In China, PV storage microgrids with EV integration have been shown to balance economic efficiency and environmental sustainability³⁷. Research in Rwanda has confirmed that PV microgrids combined with EVCS significantly reduce the levelized cost of energy (LCOE)³⁸. In Islamabad, solar-grid-tied highway charging stations reduced both costs and carbon emissions³⁹. A study in Riyadh, Saudi Arabia, demonstrated a 24% reduction in energy costs, with solar energy accounting for 77.7% of all energy consumption⁴⁰.

India's research found that an optimized HRES incorporating PVs, WTs, and EVs decreased the cost of energy (COE) to \$0.0564/kWh, enhancing overall cost-effectiveness⁴¹. In Turkey, optimization efforts at Yildiz Technical University have resulted in reduced energy costs and increased utilization of renewable energy⁴². Additional studies in India have highlighted that EVCS based on a 216-kW solar PV system can achieve a payback period of 7.21 years⁴³. Similarly, in Vietnam, PV-supported EVCS in areas with high solar radiation were found to be economically efficient⁴⁴. Lastly, in India, a combination of PV, WT, BTS, diesel generators (DG), and EVs demonstrated that the integration of PV-Grid-BTS and a converter minimized both COE and NPC, making the system cost-effective and environmentally friendly⁴⁵.

These studies collectively provide a rich foundation for advancing EVCS infrastructure. By addressing challenges such as system reliability, economic feasibility, and environmental impacts, they contribute to the growing body of knowledge on renewable energy integration into transportation systems. Their findings underscore the necessity of tailoring hybrid renewable energy system (HRES) designs to regional conditions, optimizing system configurations, and employing advanced control strategies to achieve sustainability and cost efficiency.

However, the literature reveals a critical gap in the comprehensive optimization of energy scheduling in solar-powered, grid-connected EV charging systems. Effective integration of photovoltaic (PV) energy with grid-based power sources requires precise energy management strategies to mitigate fluctuations in solar energy production. Solar energy is predominantly utilized during peak generation periods in the daytime, while grid electricity compensates during periods of low solar output, such as nighttime or under adverse weather conditions. This dual-source energy system presents unique challenges, including the alignment of energy supply with variable demand, minimization of reliance on grid power, and optimization of operational costs. Advanced optimization frameworks and scheduling algorithms are essential to address these challenges, ensuring high renewable energy penetration, enhanced system efficiency, and improved grid stability.

In response to these challenges, this study focuses on the techno-economic optimization of HRESs integrated with EV charging infrastructure. The research employs advanced simulation and modeling techniques to analyze energy flows, optimize scheduling, and design efficient system configurations. By leveraging real-world data and site-specific renewable energy potentials, the study aims to deliver practical solutions for minimizing energy costs, reducing carbon emissions, and enhancing system reliability, thereby contributing to the sustainable development of EV charging infrastructure.

Major contributions

This study makes several significant contributions to HRES and EVCS. The key contributions are as follows:

Comprehensive Analysis of Energy Potential and Requirements: This research provides a thorough analysis of the energy potential and needs of the Çukurova region to establish an EVCS. This approach identifies the high-potential RESs available in the region that can be effectively used to develop sustainable energy solutions.

- Development and Optimization of HRES: Using HOMER Pro microgrid analysis tool version 3.14.2 (https://www.homerenergy.com) software, this study develops and optimizes various HRES configurations. Six scena rios with different components, including three grid-connected and three off-grid systems, were analyzed to determine the most efficient and cost-effective configurations for the EVCS.
- Technical and Economic Evaluation: This research conducted a detailed technical and economic evaluation of
 different HRES configurations. The energy production, cost-effectiveness, and environmental impact of each
 scenario were assessed, providing valuable insights into the optimal use of RESs for EVCS.
- Environmental Impact and Sustainability: This study emphasized the environmental benefits of integrating RESs with EVCS. By reducing reliance on fossil fuels and lowering GHG emissions, this research contributes to the advancement of sustainable and environmentally friendly transportation solutions.
- Significant Cost and Emission Reductions: The study achieves a LCOE of \$0.0215/kWh, significantly reducing energy costs compared to conventional systems. Furthermore, the integration of renewable energy sources minimizes GHG emissions, demonstrating the potential of HRES to deliver both economic and environmental benefits.
- Recommendations for Implementation: Based on the findings, this study offers practical recommendations
 for the implementation of renewable energy-based EVCS in similar regions. This report highlights the best
 practices and strategies for maximizing the benefits of HRES and ensuring reliable and sustainable energy
 supply for EVs.

• Contribution to Academic and Practical Knowledge: This study bridges the gap between theoretical research and practical application. The proposed framework serves as a robust foundation for future research in the fields of HRES and EVCS, contributing to both academic knowledge and real-world energy solutions.

By addressing the technical, economic, and environmental aspects of HRESs, this study offers a comprehensive approach to enhancing the efficiency and sustainability of EV charging infrastructure.

The remainder of this paper is organized as follows: section "Mathematical foundations for hybrid renewable energy systems" provides a detailed mathematical framework for the hybrid renewable energy system. Section "Methodology" outlines the methodology of the proposed system. In section "Simulation results and discussion", the simulation results are presented along with a discussion. Finally, section "Conclusions" concludes the study by summarizing the key findings.

Mathematical foundations for hybrid renewable energy systems

Developing an effective sustainable HRES requires a solid mathematical foundation. In this section, we describe the mathematical approaches used to assess the viability, performance efficiency, and cost-effectiveness of such systems. For this purpose, HOMER Pro microgrid analysis tool version 3.14.2 software was used—a powerful optimization and simulation tool designed to model the behavior of HRES under various scenarios, was used.

Components HRES

The HRES comprises several critical components that work synergistically to provide reliable and sustainable energy. The key components are described in detail below, including their mathematical representations.

Photovoltaic (PV) panel

PV systems generate electricity from solar radiation. The most cost-effective RESs are, due to Turkey's high solar energy potential, so a 1 kW PV system was chosen for our hybrid system. The cost of 1 kW PV is \$750.00, with a renewal cost of \$750.00, a lifespan of 25 years, and operation and maintenance costs of \$10.00 per year.

The power output of the PV system (P_{PV}) and the cell temperature (T_C) can be determined using Eqs. (1) and (2) as follows⁴⁶:

$$PV_{p}\left(t\right) = \left(\frac{SR_{int}\left(t\right)}{1000}\right) \left(PV_{N}PV_{p}^{rat}W_{\eta}PV_{\eta}\right) \left(1 - \delta_{T}\left(T_{C} - T_{r}\right)\right) \tag{1}$$

$$T_C(t) = SR_{int}(t) \left(\frac{T_{nor} - 20}{800}\right) + T_A \tag{2}$$

Here, SR_{int} (t) represents the solar radiation intensity at a given time, PV_N the number of PV units, PV_p^{rat} the nominal power, W_η the wiring efficiency, PV_η the PV module efficiency, δ_T the maximum PV module temperature coefficient, T_A the ambient temperature, and T_r the reference temperature of the PV. T_{nor} represents the cell temperature under standard operating conditions, which are based on $800 \, \frac{W}{m^2}$ solar irradiance, $1 \, m/sn$ wind speed, 20 °C air temperature, and a 45° tilt angle from the horizontal⁴⁷.

Wind turbine

The WT converts the kinetic energy of the wind into mechanical energy, which is then converted into electrical energy. Owing to their high cost, the selection of turbines in the system is crucial. Several turbine models were tested in the system design, and the use of a Generic 1 kW WT was deemed appropriate. The cost of the turbine is \$500.00, with a replacement cost of \$500.00, a lifespan of 20 years, and operation and maintenance costs of \$10.00 per year. The hub height of the turbine was set to 17 m.

The wind speed varies according to the height at a specific measurement point and is measured using Eq. $(3)^{48}$:

$$\frac{v_2}{v_1} = \left(\frac{h_2}{h_1}\right)^{\alpha} \tag{3}$$

Here, v_2 represents the wind speed at the WT hub height h_2 , while v_1 is the wind speed at the anemometer height h_1 , and α is the wind shear exponent. The power output $P_{WT}(t)$ of the WT at a given wind speed v can be calculated as follows:

$$P_{WT}(t) = \begin{cases} 0 & v(t) < v_{cut-in} \\ \alpha \times v(t)^3 - b \times P_{RT_{rated}} & v_{cut-in} < v(t) < v_{rated} \\ P_{RT_{rated}} & v_{rated} < v(t) < v_{cut-off} \\ 0 & v(t) > v_{cut-off} \end{cases}$$
(4)

$$\begin{cases}
 a = \frac{P_{WT_{rated}}}{(v_{rated})^3 - (v_{cut-in})^3} \\
 b = \frac{v_{cut-in}}{(v_{rated})^3 - (v_{cut-in})^3}
\end{cases}$$
(5)

$$P_{WT_{rated}} = \frac{1}{2} \times \rho \times A_{WT} \times C_p \times (v_{rated})^3 \tag{6}$$

Here, P_{WT_rated} represents the rated power of the WT, v_{cut-in} is the wind speed at which the turbine starts generating electricity, $v_{cut-off}$ is the wind speed at which the turbine shuts down to enter safe mode, ρ is the air density, A_{WT} is the swept area of the turbine blades, and C_p is the power coefficient. The value of C_p typically ranges from 0.25 to 0.45.

Battery storage (BTS)

The BTS system converts electrical energy from the system into chemical energy for storage and then converts it back into electrical energy when needed. This component is crucial for maintaining reliable energy supply, especially when RESs are intermittent. Due to their significant cost impact, the number of Bats must be carefully considered. Based on the analysis of different battery types, a generic 100-kWh Li-Ion battery was selected. The battery cost was \$70,000.00, the replacement cost was \$70,000.00, the lifespan was 15 years, and the annual operation and maintenance cost was \$1,000.00.

The charging process of the battery can be calculated using Eq. $(7)^{49}$:

$$EBat(t) = (1 - \sigma) \times E_{Bat}(t - 1) + \left(EG(t) - \frac{EL(t)}{\eta_{conv}}\right) \times \eta_{CC} \times \eta_{rbat}$$
 (7)

Here, EBat(t) represents the energy level of the battery at time t, EBat(t-1) is the energy level of the battery at time t-1, σ is the hourly self-discharge rate of the battery, EG(t) is the generated electrical energy, EL(t) is the electrical energy demand, η_{conv} is the efficiency of the converter, η_{CC} is the efficiency of the charge controller, and η_{rbat} is the round-trip efficiency of the battery. The electrical energy generated at time t is calculated using the following equation.

$$EG(t) = [EDC(t) + EAC(t)] \times \eta conv$$
(8)

Here, $EDC\left(t\right)$ is the generated direct current (DC) energy, and $EAC\left(t\right)$ is the generated alternating current (AC) energy. They can be calculated as follows⁴⁹:

$$EDC(t) = EPv(t) + ERT(t)$$
(9)

$$EAC(t) = EBMG(t)$$
 (10)

During the discharge process, the load from the system, which generates electrical energy from the RESs, is less than the battery load and is represented as follows⁴⁹:

$$E_{bat}(t) = (1 - \sigma) \times E_{bat}(t - 1) + (E_G(t) - E_L(t) / \eta_{Conv}) - E_G(t) / \eta_{rbat}$$
(11)

System converter

The inverter (Inv) is used in the system to convert electrical power between the AC and DC forms. The system requires an AC supply for general consumption and a DC supply for charging the battery. Both AC and DC sources are essential to maintain the energy flow between the HRES components. The cost of the Inv used in the system is \$300.00, with a replacement cost of \$300.00, no annual operation and maintenance costs, a lifespan of 15 years, and an efficiency η_{inv} of 95%.

The power generated from renewable sources $P_{ren}(t)$ is expressed by the following Eq. (12)⁵⁰:

$$P_{ren}(t) = PV_P(t) + BG_P(t)/\eta_{inv}$$
(12)

Electrolyzer

The electrolyzer (Elz) is designed with two primary components: an anode and a cathode, which are separated by an electrolyte. When an electric current is passed through this electrolyte, a chemical reaction occurs, resulting in the decomposition of water into hydrogen and oxygen⁵¹. The hydrogen is then stored in a hydrogen tank (HT). For this study, the chosen electrolyzer has a lifespan of 15 years and operates at an efficiency of 85%. The capital cost per kW is \$1,500.00, the replacement cost is \$645.00, and the annual operation and maintenance expenses are \$100.00. The power transferred from the electrolyzer to the hydrogen tank, denoted as $P_{ELE/HT}$ T, is dependent on the electrolyzer's efficiency $\eta\eta_{ELE}$, while $P_{ren/ELE}$ represents the electrical energy supplied to the electrolyzer from the RES.

$$P_{ELE/HT} = \eta_{ELE}^* P_{ren/ELE} \tag{13}$$

Hydrogen tank

Following the separation of hydrogen and oxygen, hydrogen gas is transferred to an HT for storage, where it is later utilized in the fuel cell (FC) for electricity generation. To ensure stable operation, the pressure levels in the HT were regulated in accordance with the water Elz and FC pressures⁵². Hydrogen storage capacity is largely affected by winter energy demand because the tank must be capable of storing enough hydrogen produced during summer to meet the increased electricity requirements during winter. Therefore, the HT size is determined by the amount of hydrogen needed to generate sufficient electricity during colder months. In the proposed system, a 100 kg hydrogen tank is used to meet the load demands. The cost of the tank was set at \$130.00 per kilogram,

with an equivalent replacement cost, a lifespan of 25 years, and an annual operation and maintenance expense of \$10.00.

The hydrogen mass stored in the HT (HT_m) is constrained by predefined minimum and maximum limits⁵¹.

$$HT_{m}^{min} \leqslant HT_{m}\left(t\right) \leqslant HT_{m}^{max} \tag{14}$$

The energy stored in the HT $(HT_E(t))$ and the mass of hydrogen stored at time (t) $(HT_m(t))$ are expressed as follows⁵³:

$$HT_{E}(t) = HT_{E}(t - 1) + \left(P_{ELE/HT}(t) - \frac{P_{Ht/FC}(t)}{\eta_{HT}}\right) \times \Delta t$$
 (15)

$$HT_{m}(t) = HT_{E}(t)/HHV_{H}$$
(16)

In this formulation, $P_{Ht/FC}(t)$ represents the power transferred from the HT to the FC at time t, where η_{HT} denotes the efficiency of the hydrogen storage system. The variable Δt corresponds to the simulation time step, and HHV_H refers to the higher heating value of the stored hydrogen gas in kilowatt hours per kilogram (kWh/kg). These relationships are fundamental to ensure that hydrogen storage systems effectively manage energy production and consumption, thereby maintaining a stable and reliable energy supply under varying seasonal conditions.

Fuel cell (FC)

A FC is an electrochemical cell that converts hydrogen and oxygen into electricity through a redox reaction. FCs operate continuously as long as hydrogen is supplied. They produce enough electricity to meet the load demand even on the worst weather days when there is no PV production or when the battery charge level is below 40%. The cost of the FC used in the system is \$3,000.00, with a replacement cost of \$2,700.00, operation and maintenance costs of \$0.020 per hour, and a lifespan of 40,000 h.

The electrical power produced by a fuel cell (FC_P) depends on its overall efficiency (η_{FC}) and is calculated as follows⁵¹:

$$FC_P = \eta_{FC} * P_{HT/FC} \tag{17}$$

Where $P_{HT/FC}$ represents the power supplied from the HT to the FC.

Biomass gasifier

A biomass gasifier (BG) facilitates the conversion of solid biomass—such as wood, agricultural residues, or other biomass materials—into gaseous fuel via a chemical process conducted at high temperatures in an oxygendeficient environment. The system uses small-scale downdraft gasification technology, which converts solid biomass to syngas, which is subsequently utilized in turbines for electricity generation. In the Çukurova region, the average daily input of cotton and corn residues is approximately 0.4 tons. The BG system has a capital cost of \$2,500.00, a replacement cost of \$2,300.00, and operational and maintenance expenses of \$80.00 per hour. The fuel cost is \$3.5 per kilogram, and the system is designed to operate for up to 150,000 h.

The system performance is calculated as follows^{51,54,55}:

$$\eta_{sy} = \frac{LHV_{sy}m_{sy}}{LHV_{R}m_{R}} \tag{18}$$

$$BG_{p}\left(t\right) = \frac{G_{N}}{F_{m}} \left(\frac{\eta_{sy}LHV_{B}B_{rated}\left(t\right)}{LHV_{sy}} - F_{0}GP_{rat}\right)$$
(19)

$$F_{BG}\left(t\right) = \frac{LHV_{sy}}{\eta_{sy}LHV_{B}} \left(G_{N}F_{0}GP_{rat} + F_{m}BG_{p}\left(t\right)\right) \tag{20}$$

In this formulation, η_{sy} represents the efficiency of syngas production, while LHV_{sy} and LHV_B correspond to lower heating values for syngas and biomass feedstock, respectively. The variables m_{sy} and m_B denote the syngas and biomass mass flow rates, respectively. The electrical output power generated by the biomass gasifier at any given time t is expressed as $BG_p(t)$, with G_N indicating the number of generators operating in the system. The hourly biomass consumption rate is represented by $B_{rated}(t)$, while the rated power of the generator is denoted as GP_{rat} . Furthermore, the term $F_{BG}(t)$ signifies the average hourly fuel consumption, with F_m representing the marginal fuel consumption rate and F_0 indicating the no-load fuel consumption factor.

GHG emissions from feedstock can be calculated as follows⁵¹:

$$BE_T = LHV_B *Sum (B_{rated})$$
(21)

$$E_{Con} = BE_T *0.0002778 (22)$$

$$GHG = E_{Con} * GWP * 0.43$$
(23)

The total biomass consumption (BE_T) is calculated as shown in Eq. (21). The energy consumption (E_{Con}) is then determined using Eq. (22). Finally, the GHG emissions (GHG) are calculated using Eq. (23), where BE_T

represents the total biomass consumption, E_{Con} represents the energy consumption in kWh, GWP is the global warming potential (GWP = 1), and 0.43 is the electricity emission factor in kg CO₂/kWh.

Electrical vehicle charge station (EVCS)

EVs operate differently from traditional internal combustion engine vehicles by transmitting power to the wheels using electrical energy generated by one or more electric motors. This power allows vehicle movement. EVs come in various types, including battery electric vehicles (BEVs), hybrid electric vehicles (HEVs), and plugin hybrid electric vehicles (PHEVs). BEVs operate solely on electric motors and are powered exclusively by the BTS. These vehicles typically use large batteries, and battery capacity is a crucial factor affecting vehicle range. Advances in technology have increased battery capacities, thereby extending the range of EVs.

HEVs combine internal combustion engines with electric motors, and use energy from both sources to power the vehicle. Hybrid vehicles aim to reduce fuel consumption and emissions by using an electric motor alongside an internal combustion engine. PHEVs, on the other hand, use a BTS and electric motors in addition to internal combustion engines. These vehicles can operate on electric power for short distances, with the internal combustion engine activated for longer trips to extend the range. PHEVs are designed to overcome the range limitations of EVs, providing greater flexibility.

EVs offer an environmentally friendly alternative that reduces the dependency on fossil fuels and lower GHG emissions, significantly contributing to sustainable transportation systems. They also boast high energy efficiency, low operating costs, and provide quiet driving experience⁵⁶. As the demand for energy increases with EV charging, the load on the grid becomes significant, necessitating the optimization of electricity transmission and distribution systems to maintain a balance between supply and demand.

With the widespread adoption of EVs, the importance of EVCS has increased. These stations provide the necessary infrastructure to recharge EV batteries. Charging stations can vary in power levels; home charging stations offer lower power levels, while fast charging stations can deliver higher power levels and recharge BTS more quickly⁵⁷. The number of charging stations is increasing, and they are easily accessible in public places, parking lots, and along roadsides.

The consumed energy by EVs can be calculated as follows⁵⁸:

$$P_c = \frac{K_d E_k}{t} \tag{24}$$

where K_d is the number of kilometers driven, E_k is the energy required to drive the vehicle, and t is the time required to charge the vehicle.

To calculate the consumed energy by the electric vehicle, the following equation is used⁵⁸:

$$P_C = Q_{batch} \times \frac{((SOC_{max}) - SOC)}{t} \tag{25}$$

where Q_{batch} is the battery capacity, SOC_{max} is the maximum state of charge, SOC is the state of charge, and t is the time required to charge the vehicle.

The total consumed power by all vehicles can be expressed as follows⁵⁸:

$$P = \sum_{i=1}^{N} P_C \tag{26}$$

This comprehensive framework ensures efficient calculation and management of energy consumption for EVCS, highlighting the importance of optimizing charging infrastructure to support the growing adoption of EVs.

Cost evaluation and component modeling

This section of the study focuses on a detailed cost analysis that incorporates mathematical modeling of expenditures related to energy production, consumption, and grid integration. In addition, it includes simulations to evaluate energy demand and the interaction between the grid and renewable energy sources. The main aim of this section is to establish a comprehensive framework for assessing the financial aspects of HRES. The mathematical formulations presented here are crucial for accurately estimating the costs associated with different system components, particularly in the context of load management and grid connectivity.

Furthermore, the cost evaluation process examines the capital expenditures (CAPEX), operating expenses (OPEX), and the replacement costs of various system components, including energy storage, converters, and inverters. Integrating these factors into a unified model provides a holistic understanding of the system's economic viability. Special attention should be given to the influence of fluctuating energy demands, seasonal variations, and the integration of multiple energy sources, such as PV systems and biomass gasifiers, on the overall cost structure.

Additionally, this analysis seeks to optimize the balance between initial capital investments and long-term operational efficiency. The results of this evaluation will inform decision-making related to system scalability, potential cost reductions, and strategic resource deployment to improve financial performance over the system's lifespan.

Cost analysis

The NPC represents the present value of a project or investment and encompasses various factors, such as capital cost, operation and maintenance costs, replacement cost, salvage value, and payback period. The NPC was calculated using the following equation⁶:

$$NPC = \frac{C_{ann,tot}}{CRF\left(i, R_{proj}\right)} \tag{27}$$

where the capital recovery factor (CRF) is defined as follows⁶:

$$CRF_{(i,N)} = i(1+i)^n/(1+i)^{(n-1)}$$
 (28)

In these equations, $C_{ann,tot}$ represents the total annual cost, CRF is the capital recovery factor, i is the interest rate, and \hat{R}_{proj} is the project lifetime.

These calculations ensure a comprehensive evaluation of the project's financial feasibility by accounting for all associated costs and present value, providing a clear metric for investment decision-making.

The LCOE is a measure of the total NPC of energy production per unit of generated energy. It is used for investment planning and for making consistent comparisons between different energy generation methods. The LCOE was calculated using the following equation⁵⁹:

$$LCOE = \frac{C_{ann,tot} - C_{boiler} \times H_{served}}{E_{served}}$$
 (29)

Here, the total annual cost of the system $(C_{ann,tot})$ is expressed in dollars per year, the marginal cost of the boiler (C_{boiler}) is in dollars per kilowatt-hour, the total thermal load served (H_{served}) is measured in kilowatt-hours per year, and the total electrical load served (E_{served}) is also in kilowatt-hours per year.

The capital cost of an HRES includes the costs of components and installation. Then, it can be calculated using Eq. $(30)^{60}$:

$$C_{ACC}^{RT} = C_{cap}^{RT} \times CRF(i, n)$$
(30)

where $C_{ACC}^{\ RT}$ represents the initial cost of the WT and CRF is the capital recovery factor.

The replacement cost is the cost of replacing a component at the end of its useful life, calculated as follows⁶⁰. Where C_{rep}^{RT} is the replacement cost.

$$C_{Arep}^{RT} = C_{rep}^{RT} \times CRF(i, n) \times 1/(1+i)^{y}$$
(31)

The salvage value is defined as the remaining value of the component at the end of the project's life. The WT can then be calculated as follows:

$$C_{sal}^{RT} = C_{rep}^{RT} \times (R_{return}/(N_{wind.1}))$$
(32)

where R_{return} is the lifecycle of the remaining WT, and $N_{wind.1}$ is the lifespan of the WT.

The capacity factor is the ratio of the actual energy produced by the system over a year (running 24 h a day) to the maximum possible output under nominal power over the same period. It is calculated as follows⁶⁰:

$$CF(\%) = \frac{E_{ac}}{P_0 \times 24 \times 365} \times 100$$
 (33)

where E_{ac} is the actual energy output, and P_0 is the nominal power output.

Methodology General framework

The primary objective of this study is to reduce the dependency on fossil fuels and enhance the integration of RES into EVCSs and building infrastructure through the implementation of HRES. Using HOMER Pro microgrid analysis tool version 3.14.2 software, this study focuses on increasing the share of renewable energy within local EVCSs and buildings to minimize carbon footprints and reduce CO2 emissions. The optimization approach incorporates not only solar and wind energy, but also strategic interactions with the grid, enabling effective management of energy transactions, including purchases and sales, as needed.

In this study, the Çukurova region of Adana province (37°5.9'N, 35°8.9'E), one of Turkey's most sulfitic regions, was selected as the research site. Initially, a comprehensive literature review was conducted to gather information on renewable energy systems, EVCS, HOMER Pro microgrid analysis tool version 3.14.2 simulation software, and optimization methods. Subsequently, a unique electrical load profile was developed for the Çukurova region, and energy production and consumption models for various scenarios were created. The region's average wind speed, temperature, and solar radiation data were obtained from the Turkish Ministry of Environment, Urbanization, and Climate Change's General Directorate of Meteorology and used as inputs for the simulations.

The methodology explored different configurations of renewable energy systems. These systems included components such as the PV panel, BG, WT, HT, Elz, FC, Bat, and Inv. Six distinct scenarios, each with varying

system components, were developed to evaluate the performance of the energy systems. The scenarios are as follows:

- Scenario 1: PV, BG, HT, Elz, FC, Bat, and Inv.
- Scenario 2: PV, WT, Bat, and Inv.
- Scenario 3: PV, WT, HT, Elz, FC, Bat, and Inv.
- Scenario 4: PV, BG, HT, Elz, FC, Bat, Inv, and Grid.
- · Scenario 5: PV, WT, Inv, and grid.
- Scenario 6: PV, WT, HT, Elz, FC, Bat, Inv, and Grid.

The primary focus of this study was to identify the optimal configurations to meet the energy demands of EVCSs while maximizing their energy efficiency and sustainability. To achieve this, HOMER Pro microgrid analysis tool version 3.14.2 simulation software was used to analyze the energy production and consumption data under different scenarios. The goal was to determine the most suitable HRES configurations for EVCS in the Çukurova region of Adana. This study aims to contribute significantly to the planning of energy systems and sustainable development strategies in the region by evaluating the performance of different scenarios and conducting optimization analyses using HOMER Pro microgrid analysis tool version 3.14.2 software.

Figure 1 illustrates the workflow of the methodology as a process flow diagram.

1. Input phase:

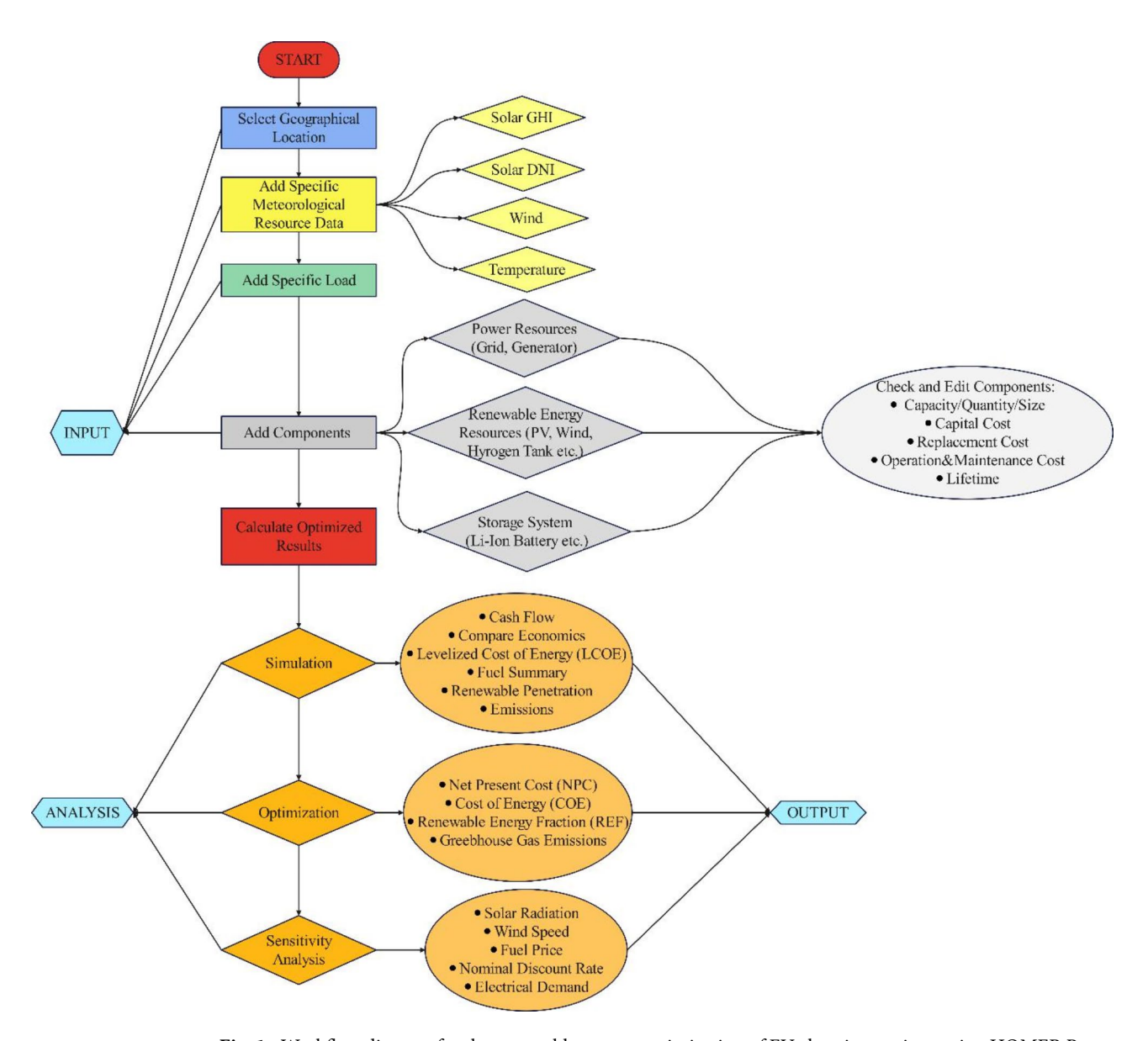


Fig. 1. Workflow diagram for the renewable energy optimization of EV charging stations using HOMER Pro microgrid analysis tool version 3.14.2 software.

- Select Geographical Location: The Çukurova region of Adana was selected.
- Additional Specific Meteorological Resource Data: Solar GHI, Solar DNI, Wind, and Temperature data were obtained and inputted.
- Add Specific Load: A unique electrical load profile for the region was developed.
- Add Components: The system components, including Power Resources (Grid, Generator), Renewable Energy Resources (PV, Wind, Hydrogen Tank, etc.), and Storage Systems (Li-Ion Battery, etc.), were added.
- Check and Edit Components: This includes adjusting the capacity/quantity/size, capital cost, replacement cost, operation and maintenance cost, and Lifetime of each component.

2. Calculation phase:

 Optimized Results: The optimized results were calculated using HOMER Pro microgrid analysis tool version 3.14.2.

3. Analysis phase:

- Simulation: This includes Cash Flow analysis, Economic Comparison, LCOE, Fuel Summary, Renewable Penetration, and emission analyses.
- Optimization: This covers NPC, LCOE, renewable energy fraction (REF), and GHG emissions.
- Sensitivity Analysis: Factors such as Solar Radiation, Wind Speed, Fuel Price, Nominal Discount Rate, and Electrical Demand were analyzed for their impact on the system.

By systematically following these steps, this study determined the most efficient and sustainable HRES configuration for EVCS in the Çukurova region, as summarized in Table 1. The results of this research provide valuable insights into the planning and optimization of renewable energy systems, contributing to a broader goal of sustainable energy development.

HOMER pro simulation of HRES

HOMER Pro is reliable software widely used for the sizing and optimization of multiple energy sources, also known as a hybrid optimization program. The software assists in performing preliminary feasibility tests and conducting sensitivity analyses for various configurations of the desired energy systems. The software was developed by the US National Renewable Energy Laboratory (NREL) for grid-connected and off-grid applications. It runs on the Windows platform and is programmed in $C++^{46}$.

Designing and configuring a microgrid involves critical decision-making regarding component sizing, component design, and selecting a suitable location. The inflation rate, interest rate, and other technical specifications of the selected components are necessary for the cost assessment of these hybrid energy systems. Regarding decision making, there are many choices depending on the technology used and the availability of energy sources. The HOMER Pro platform integrates both optimization and sensitivity algorithms, thus streamlining the evaluation process. Optimal simulations adhere strictly to user-specified constraints, targeting the minimal NPC value. Beyond performing energy balance assessments, HOMER Pro filters out infeasible designs, spotlighting viable configurations that guide users in determining the ideal system blueprint. Moreover, this simulation rigorously examines a system's technical viability, ensuring that it addresses both electrical and thermal demands within the set constraints. The platform also delves into the system's NPC, factoring in costs related to installation and ongoing maintenance. Spanning a full year, or 8760 h, HOMER Pro's simulation yields results in a structured table, supplemented with illustrative graphs and charts. These visuals delineate technical and economic metrics, elucidate the techno-economic dynamics, and permit comparison across hybrid energy system designs. The output is export-ready for deeper analysis. The core elements of the optimization include decision parameters such as PV dimensions, WT count, battery numbers, converter capacity, inclusion of renewable resources such as PV arrays and WTs, generator magnitude, and a dispatch blueprint dictating operational strategies.

Figure 2 provides a comprehensive flowchart detailing each phase of the HOMER Pro simulation process. The simulation incorporates key economic parameters, including a nominal discount rate of 19%, an inflation

rate of 17%, and a project lifetime of 25 years, ensuring a realistic cost assessment. The geographic configuration for the Çukurova region is precisely defined using HOMER Pro's mapping tools, and the system components,

Component	Capacity	Capital cost	Replacement cost	Operation and maintenance costs	Lifetime
Solar panel	1 kW	\$750.00	\$750.00	\$10.00	25 years
Wind turbine	1 kW	\$500.00	\$500.00	\$10.00	20 years
Biomass Gasifier	500 kW	\$2,500.00	\$2,300.00	\$80.00/hour	150,000 h
Battery	1 kWh	\$700.00	\$700.00	\$10.00	15 years
Inverter	1 kW	\$300.00	\$300.00	\$0.00	15 years
Hydrogen tank	1 kg	\$130.00	\$130.00	\$10.00	25 years
Electrolyzer	1 kW	\$1,500.00	\$645.00	\$100.00	15 years
Fuel cell	1 kW	\$3,000.00	\$2,700.00	\$0.020/hour	40,000 h

Table 1. Cost and lifetime specifications of HRES components.

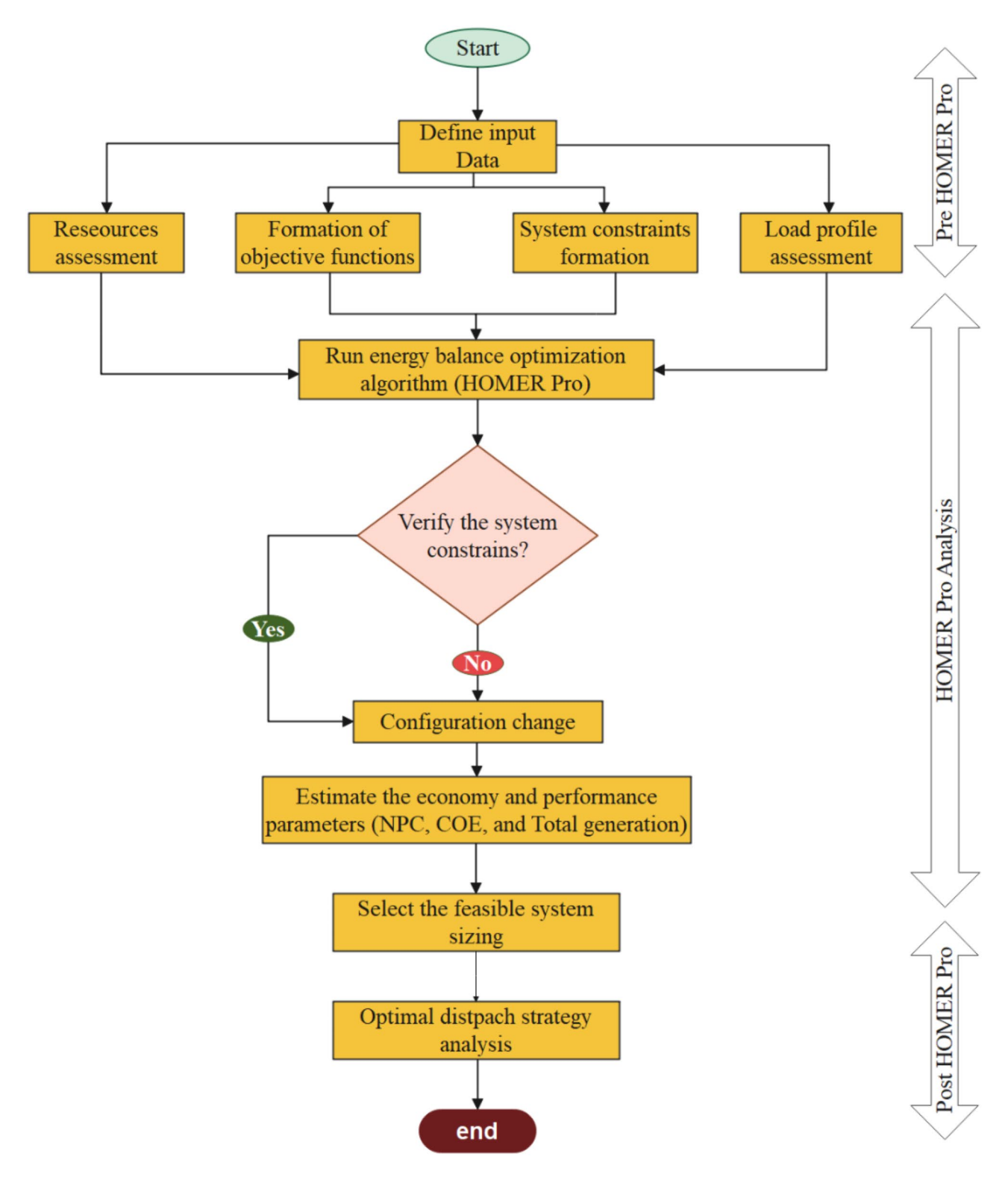


Fig. 2. HOMER Pro optimization flow diagram.

including PV, biomass gasifier, hydrogen tank, and batteries, are optimized to align with regional renewable energy potential.

In this study, the Load Following (LF) and Cycle Charging (CC) dispatch strategies were evaluated to determine their effectiveness in optimizing HRES for EVCS. These strategies, integral to HOMER Pro's optimization framework, adopt distinct approaches to energy management by balancing operational costs, resource efficiency, and system reliability. The LF strategy focuses on meeting primary loads by producing only the required energy in real time, thereby minimizing fuel consumption and operational expenses. Secondary

objectives, such as battery charging or deferred loads, are addressed primarily through renewable energy sources, reducing generator dependency and enhancing cost efficiency. In contrast, the CC strategy operates generators at full capacity during activity, with excess energy directed toward charging storage systems or deferred loads. While this ensures optimal generator utilization and increases system resilience during peak demand periods, it also results in higher fuel consumption and operating costs. Simulation results demonstrated that the LF strategy consistently provided superior economic performance under the studied scenarios, achieving reduced operating costs and improved financial feasibility by prioritizing real-time load demands and minimizing unnecessary energy production. Although the CC strategy was advantageous in scenarios requiring intensive storage use, its elevated operational costs rendered it less effective for the conditions analyzed. These findings emphasize the importance of selecting dispatch strategies tailored to specific operational contexts, resource availability, and load profiles, offering valuable insights for the efficient deployment of HRES in EVCS infrastructure.

Meteorological and electrical load data

For this study, the Çukurova region of Adana province (37°5.9′ N, 35°8.9′ E), one of Turkey's most slanted regions with developed industrial and agricultural sectors, was selected (Fig. 3 illustrates the study area). The Çukurova region not only has a high potential for solar energy but also serves as a hub for agricultural activities. This makes it feasible to establish biomass gasification or biomass energy systems that convert agricultural waste into energy. Using agricultural waste for energy production supports sustainability by converting waste into valuable resources. The diversity of RESs in this region makes it an ideal candidate for hybrid systems to ensure continuous energy supply.

Meteorological data for the Çukurova region of Adana were obtained from the General Directorate of Meteorology under the Ministry of Environment, Urbanization, and Climate Change in Turkey (Fig. 4). According to these data, the average annual solar radiation was 4.54 kWh/m²/day, the average wind speed was 2.69 m/s, and the average temperature was 19.73 °C. These meteorological values were directly incorporated into the simulation to ensure realistic and region-specific results.

The demand profile for the Çukurova region's EVCS load was based on real-world data obtained from the Ministry of Energy and Natural Resources of the Republic of Turkey. Hourly load data covering a full year (8760 h) accurately represented the total demand of existing charging stations in the region. The load profile for the Çukurova region was designed based on the hours of peak energy demand within the community. The average daily energy consumption was 1179.00 kWh/day, peaking at 160.1 kW. The analysis of the daily profile revealed that the energy demand peaked around 18:00, with an average consumption of 92.56 kW.

The monthly profile indicates that average demand is higher in August than in other months as in Fig. 5. This detailed analysis of both hourly and monthly demand variations ensures that the simulation aligns with real-world energy usage patterns in the Çukurova region, providing a robust basis for evaluating the proposed hybrid energy systems.

The grid electricity cost parameters used in this study were based on the tariff rates provided by the Ministry of Energy and Natural Resources of the Republic of Turkey. The electricity purchase cost from the grid was set

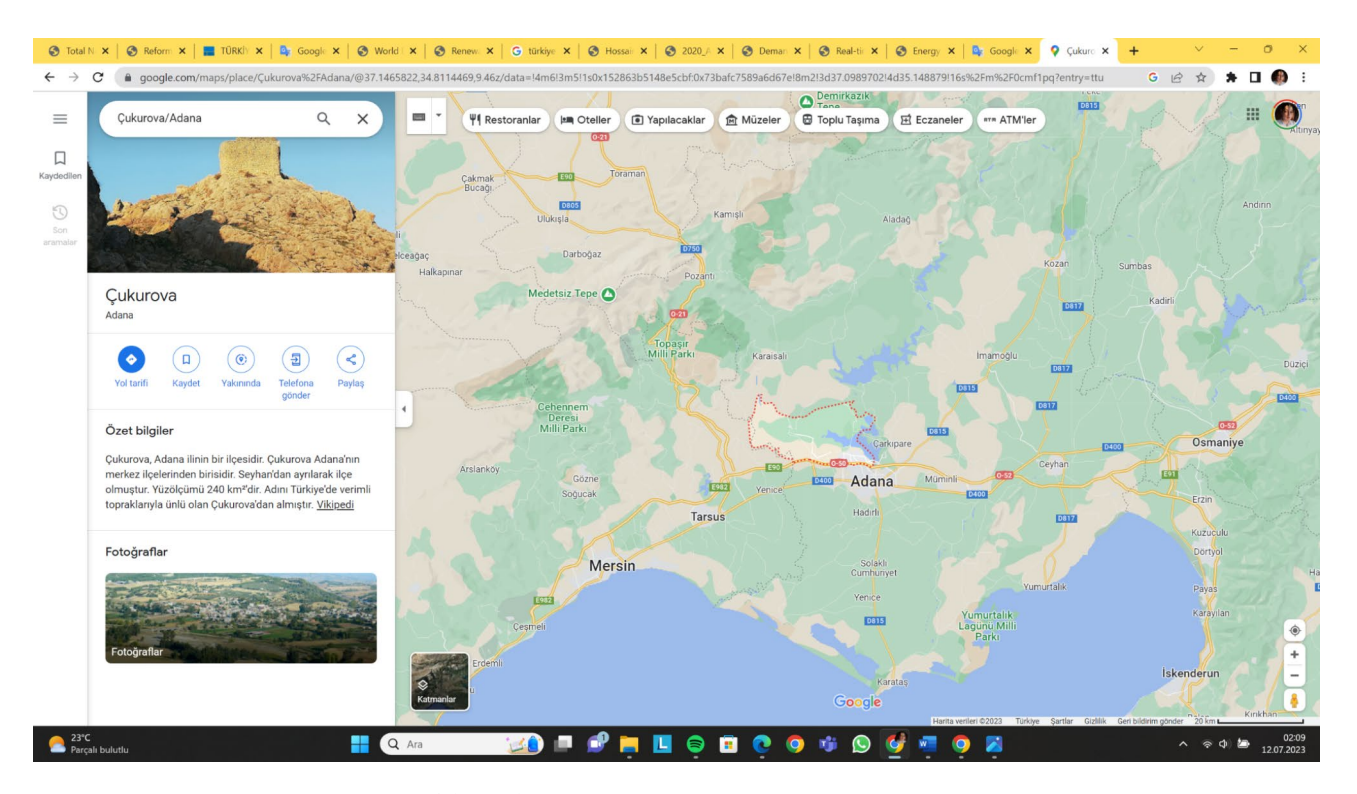


Fig. 3. Location of the study.

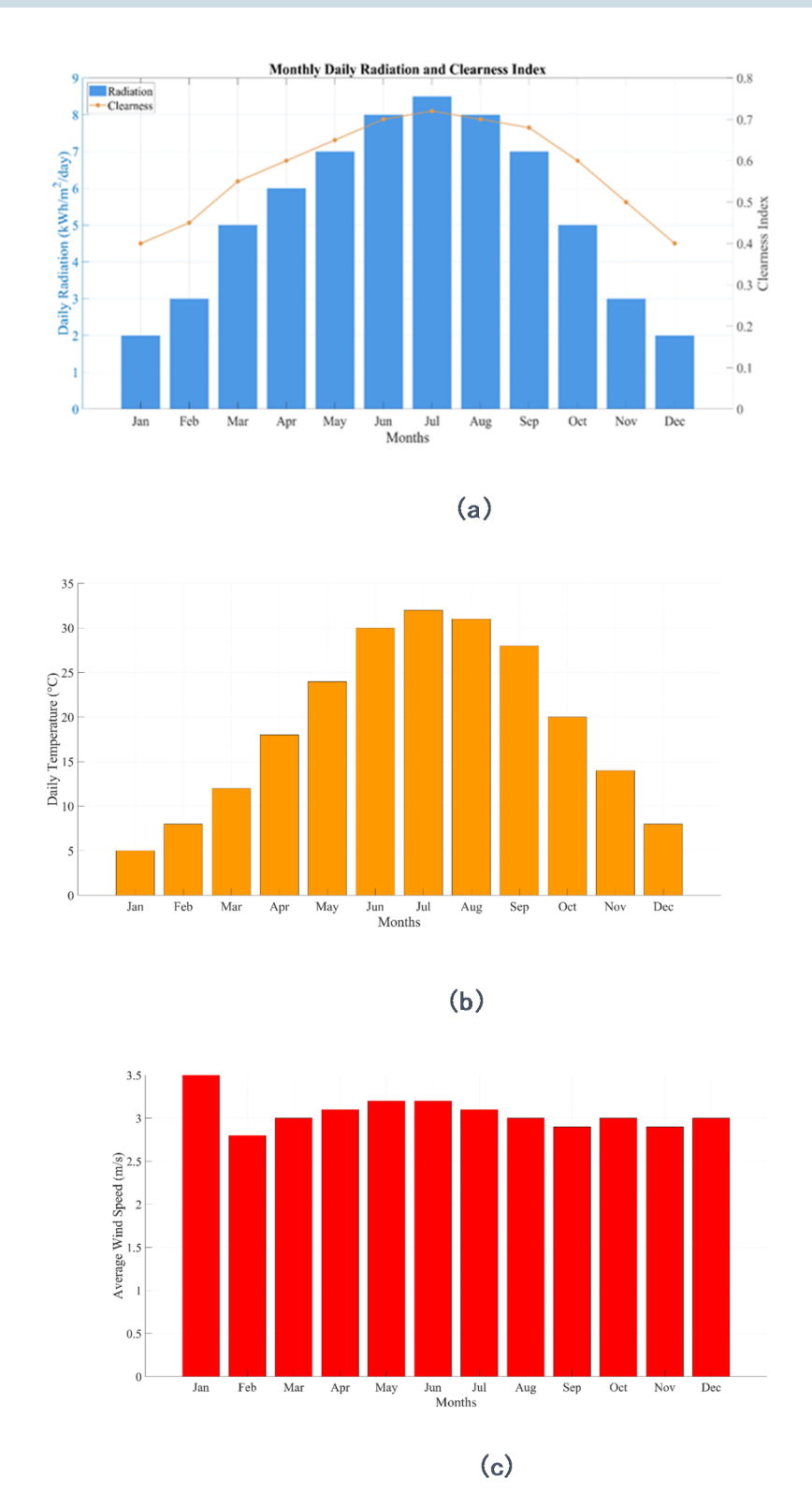


Fig. 4. Meteorological data for the study site: (a) solar radiation, (b) ambient temperature, and (c) wind speed.

at \$0.35/kWh, while the sellback price for renewable energy exported to the grid was assumed to be \$0.15/kWh. These values were incorporated into the simulation to reflect the regional economic context and ensure accurate cost modeling.

Proposed system architecture for the scenarios

In this study, we aimed to optimize the configuration and performance of hybrid RESs in the Çukurova Region. The system architectures of the scenarios are illustrated in Figs. 6 and 7, and 8.

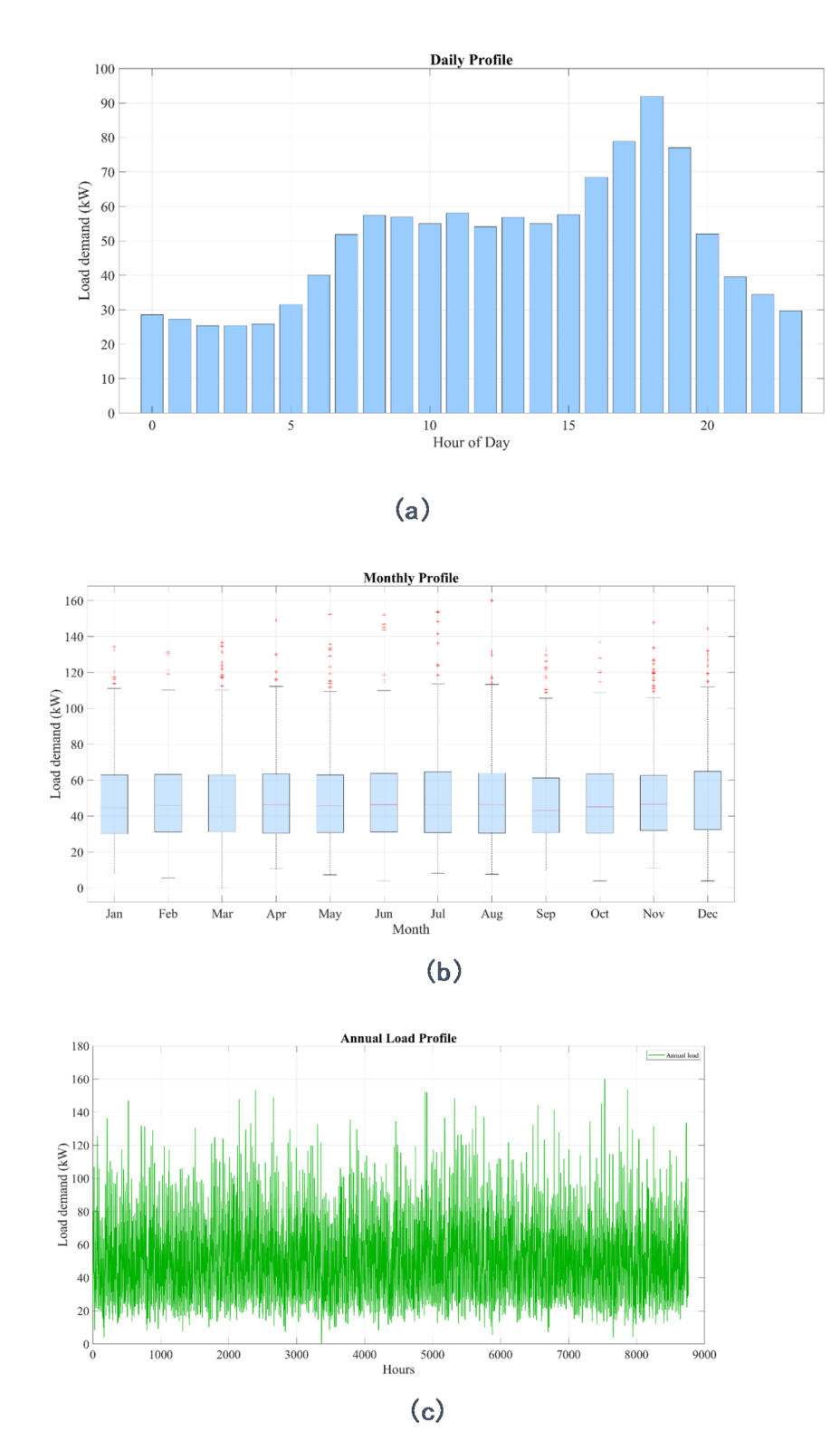


Fig. 5. Load profiles (a) daily, (b) monthly, and (c) annually.

Figure 6 illustrates Scenarios 1 and 2, which include various combinations of components such as a diesel generator, biomass generator, PV panels, FC, Bat, and Elz. Scenario 1 is notable for its integration of an HT and an electrolyzer, whereas Scenario 2 enhances the energy diversity by incorporating both WT and PV panels. Figure 7 presents Scenarios 3 and 4, which represent more complex system configurations. Scenario 3 employs an HT for storage, while Scenario 4 enhances energy security by integrating the HT with the electrical grid. These scenarios maximize the use of renewable energy by integrating WT and PV panels alongside Elz and FC. Figure 8 shows Scenarios 5 and 6, which are the most comprehensive system configurations. Both scenarios

Scenario 1 Scenario 2 Hydrogen Tank DC **Electric Load Diesel Genset PV Panel** DC **Diesel Genset** Electric Load Electrolyzer 1179.00 kWh/d 160.10 kW peak Batter Wind Turbine Converter 1179.00 kWh/d 160.10 kW peak **Fuel Cell Biogas Genset** Converter **PV Panel** Battery

Fig. 6. Single-line diagrams of hybrid renewable energy configurations for scenarios 1 and 2.

involve combinations of the electrical grid, WTs, diesel generators, PV panels, Bat, and Elz. In addition, Scenario 6 includes an HT, which increases the use of RESs and the system's storage capacity.

The comparative analysis of these scenarios evaluates their energy production and storage capacities, cost-effectiveness, and environmental impacts. Through simulations and optimization studies, the most advantageous scenarios in terms of energy efficiency and sustainability were identified. These findings provide valuable insights into the design and implementation of HRES and enhance energy supply security in the region. Consequently, the most suitable HRES configurations for the Çukurova Region were identified, leading to strategic recommendations for the effective use of RESs.

Simulation results and discussion

This section presents the detailed simulation results for each scenario. The results encompass the total energy production, cost analysis, and operational performance of each component in the hybrid energy system. The analysis provides a comprehensive understanding of the efficiency, economic feasibility, and environmental impact of the proposed scenarios.

As illustrated in Table 2, Scenario 1's PV system has a maximum output power of 622 kW with a penetration rate of 164%, highlighting its efficiency by producing more electricity than consumed and operating for 3,389 h annually with an LCOE of \$0.0466/kWh. In contrast, Scenario 2, which is also detailed in Table 2, enhances the renewable mix by incorporating a WT with a maximum output power of 672 kW, a penetration rate of 24.9%, and a capacity factor of 4.58%, along with an 861-kW PV system with a penetration rate of 221%.

As shown in Table 3, Scenario 3's PV system has a lower maximum output power of 545 kW and a penetration rate of 140%, paired with a WT that generates 585 kW at a penetration rate of 54.6% and a CF of 4.58%. This scenario's electrolyzer operates for 1,591 h annually, producing 257 kg of hydrogen with a CF of 13.6%. In contrast, Scenario 4, as shown in Table 3, achieved the highest PV output power of 1,053 kW with a penetration rate of 277%, and BG generated 48,294 kWh/year at an efficiency of 31.0%.

According to Table 4, Scenario 5 features a PV system output power of 1,076 kW with a penetration rate of 277%, which is notably supported by a WT with a substantial maximum output power of 10,000 kW and a penetration rate of 933%, although the CF is 4.58%. Scenario 5's inverter manages 1,160,927 kWh/year of energy input and output, and it manages 1,102,881 kWh/year. Scenario 6, also highlighted in Table 4, mirrors Scenario 5 in terms of PV and WT specifications, but its electrolyzer produces 300 kg of hydrogen annually over 1,263 h, resulting in a CF of 15.9%. The FC in Scenario 6 operates for 8,361 h per year and has a lifespan of 4.78 years.

These scenarios demonstrate various energy storage capabilities and operational efficiencies. For instance, Scenario 1's BTS offers 21.2 h of autonomy and a 14-year lifespan, while Scenario 6's BTS provides 14.7 h of autonomy and a 15-year lifespan. Emission results and energy procurement also vary, with Scenario 3 demonstrating negative CO₂ emissions of -1.65 kg/year, indicating environmental benefits, whereas Scenario 4 records significantly higher CO₂ emissions of 165,640 kg/year due to biomass consumption. Furthermore,

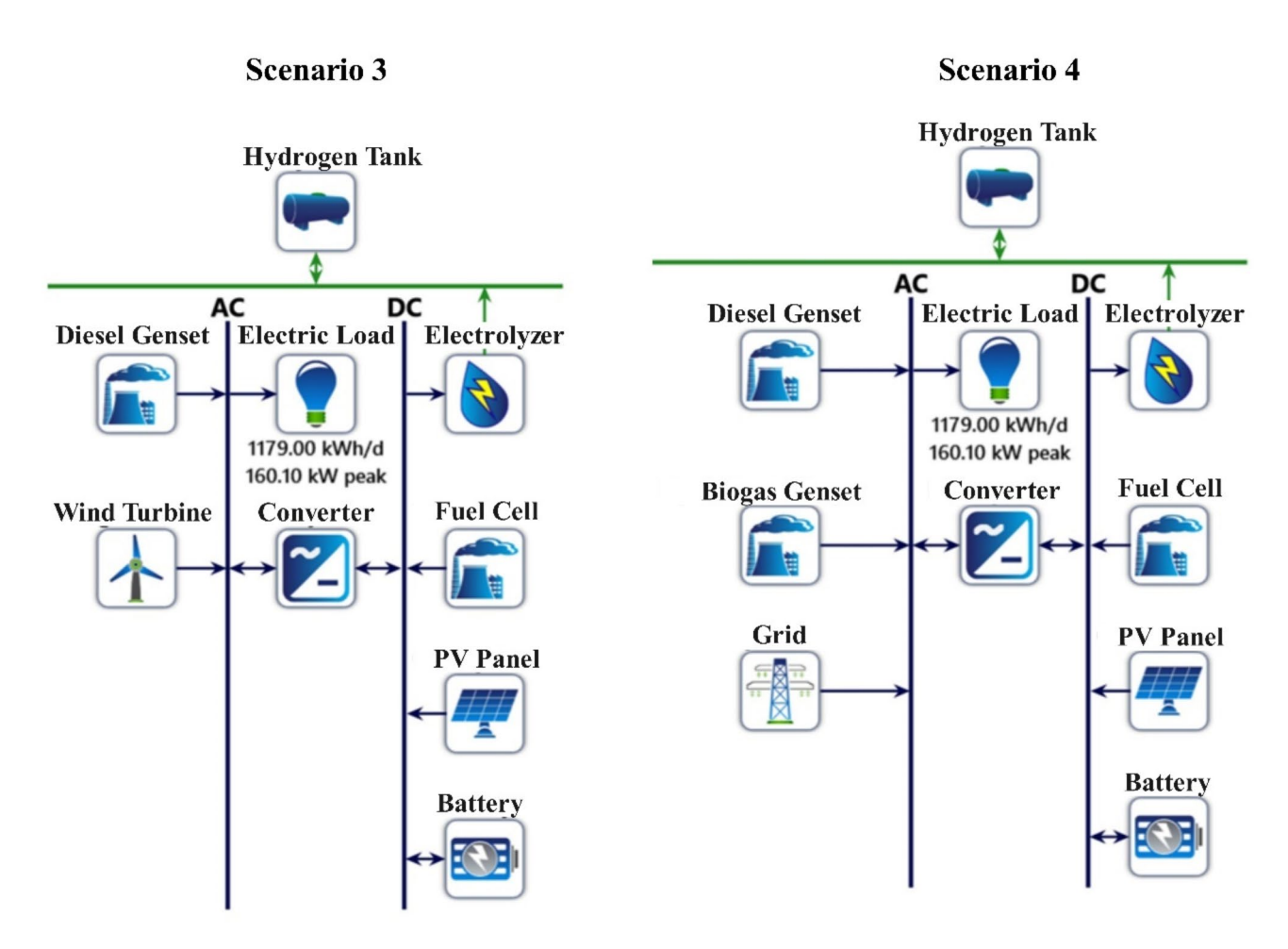


Fig. 7. Single-line diagrams of hybrid renewable energy configurations for scenarios 3 and 4.

energy procurement and sales differ notably, with Scenario 5 achieving the highest net-sold energy of 4,688,909 kWh, generating \$13.7 million in revenue, and Scenario 6 closely following, with net-sold energy of 4,656,382 kWh and revenue of \$13.8 million.

The comparative analysis provided by Fig. 9a and b, and c offers a holistic evaluation of the scenarios based on energy production, total cost, and cost efficiency, highlighting the interplay between technical performance and economic feasibility in HRES designs.

Figure 9a underscores the energy production capabilities of each scenario, with Scenarios 5 and 6 achieving the highest output due to their reliance on extensive WT installations and large-scale PV systems. The significant contributions of wind energy in these scenarios showcase the potential for high renewable energy penetration in grid-connected systems. However, their dependence on external grid infrastructure for balancing energy generation and consumption raises concerns about energy reliability in off-grid or isolated settings, making them less favorable for applications where grid independence is a priority. Scenario 4, while producing less energy than Scenarios 5 and 6, demonstrates a strategic combination of PV and biomass gasification, complemented by hydrogen-based storage technologies, to provide a more localized and balanced energy supply. Figure 9b highlights the total cost implications of each scenario, revealing distinct trade-offs between upfront investment and operational expenses. Scenarios 5 and 6 exhibit negative total costs due to substantial revenue from grid energy sales, demonstrating the economic viability of high-production, grid-tied systems. However, these scenarios rely heavily on grid interaction, which, while economically advantageous, may introduce operational challenges such as grid congestion or dependency on external energy markets. In contrast, Scenario 4 achieves a more sustainable total cost by leveraging biomass as a dispatchable renewable energy source, minimizing grid reliance while maintaining economic competitiveness. Its ability to meet energy demands without overburdening the grid underscores its suitability for regions with intermittent renewable resources or limited grid infrastructure. Figure 9c delves into the cost efficiency of the scenarios, further validating the insights from Fig. 9a and b. Scenarios 5 and 6 achieve negative cost values due to their high net energy sales; however, these configurations may not be practically implementable in areas without robust grid support. Scenario 4, on the other hand, emerges as the most cost-efficient option among the implementable configurations, balancing economic feasibility with technical reliability. By integrating PV, biomass, and hydrogen technologies, Scenario 4 ensures energy sustainability while maintaining cost efficiency, addressing the dual challenges of rising energy demands and environmental constraints.

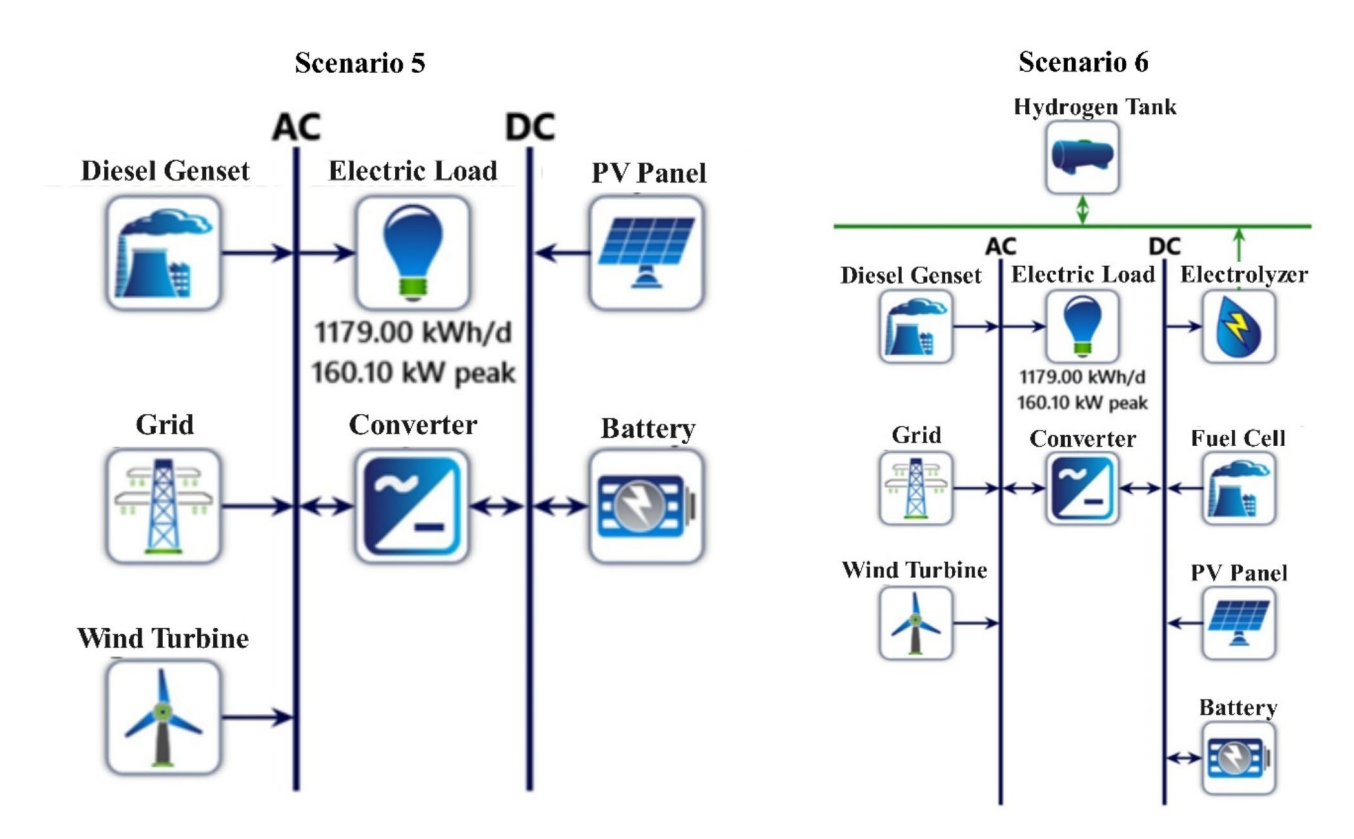


Fig. 8. Single-line diagrams of hybrid renewable energy configurations for scenarios 5 and 6.

	Scenario1			Scenario2			
Component	Size	Energy production (kWh/year)	Total cost (\$)	Size	Energy production (kWh/year)	Total cost (\$)	
Solar panel	542 kW	705,036	663,655	861 kW	952,445	898,747	
Wind turbine	-	-	-	267 kW	107,237	217,027	
Biomass Gasifier	250 kW	46,250	300,093		-	-	
Electrolyzer	10.0 kW	10,757	38,801		-	-	
Hydrogen tank	87 kg	3,333	33,206		-	-	
Fuel cell	0.400 kW	2,300	4,430		-	-	
Battery	1120 kWh	278,916	1,760,000	1100 kWh	247,050	1,540,000	
Converter	160 kW	423,660	74,660	160 kW	351,094	75,039	
System total		753,586	2,880,000	-	1,059,681	2,730,000	

Table 2. Costs and energy production of system components for scenario 1 and 2.

Collectively, these figures emphasize the importance of a balanced approach in HRES design, where energy production, cost dynamics, and operational practicality must align with regional energy goals. Scenario 4 exemplifies this balance, showcasing how hybrid systems can optimize renewable energy integration, enhance grid stability, and reduce dependency on fossil fuels, paving the way for scalable and economically viable energy solutions.

The NPC and LCOE values indicate that Scenario 4, which integrates a PV-BG-HT-Elz-FC-Inv grid, is the most viable system configuration. As illustrated in Table 5, Scenario 4 presents the lowest LCOE of \$0.0215 per kWh, which significantly outperforms the other scenarios in terms of cost efficiency. This superior performance is primarily due to the effective harnessing of solar, biomass, and hydrogen energy sources within a grid-connected hybrid system in the Çukurova region. The substantial reduction in energy costs coupled with the system's ability to generate more energy than it consumes underscores its sustainability and economic feasibility. Therefore, Scenario 4 not only offers the most cost-effective solution but also demonstrates a high potential for sustainable energy production, making it the most practical choice for implementation in similar geographical areas. This analysis reaffirms the strategic advantage of adopting a diversified energy approach to meet future energy demands both sustainably and economically.

	Scenario3			Scenario4		
Component	Size	Energy production (kWh/year)	Total cost (\$)	Size	Energy production (kWh/year)	Total cost (\$)
Solar panel	545 kW	603,322	569,307	136 kW	1,193,484	1,120,000
Wind turbine	585 kW	234,957	475,508		-	-
Biomass gasifier	-	-	-	500 kW	48,294	170,753
Electrolyzer	10.0 kW	11,927	38,801	10.0 kW	13,931	38,801
Hydrogen tank	95.1 kg	3,333	33,206	99.7 kg	3,333	33,206
Fuel cell	0.400 kW	2,698	5,187	0.400 kW	3,341	6,260
Battery	110 kWh	222,009	1,430,000	-	-	-
Converter	143 kW	304,244	66,897	723 kW	1,154,685	337,779
Grid	-	-	-	974.141 kWh	262,050	- 1,110,000
System total	•	840,977	2,620,000	-	1,507,169	603,951

Table 3. Costs and energy production of system components for scenario 3 and 4.

	Scenario5			Scenario6			
Component	Size	Energy production (kWh/year)	Total cost (\$)	Size	Energy production (kWh/year)	Total cost (\$)	
Solar panel	1076 kW	1,190,556	1,120,000	1076 kW	1,190,556	1.120,000	
Wind turbine	10,000 kW	4,016,364	8,130,000	10,000 kW	4,016,364	8.130,000	
Biomass gasifier	-	-	-	-	-	-	
Electrolyzer	-	-	-	10.0 kW	13,940	38,801	
Hydrogen tank	-	-	-	99.7 kg	3,333	33,206	
Fuel cell	-	_	-	0.400 kW	3,344	6,266	
Battery	-	-	-	900 kWh	117,093	10,228	
Converter	723 kW	1,160,927	337,779	723 kW	1,244,140	337,779	
Grid	4,807,321 kWh	118.412	- 13,700,00	4,744,646 kWh	88.264	- 13.800,000	
System total		5,325,331	- 4,140,000		5,298,528	-4.080,000	

Table 4. Costs and energy production of system components for scenario 5 and 6.

Operational challenges, particularly maintenance requirements for biomass gasifiers and hydrogen tanks, play a critical role in determining the long-term viability of HRES. Biomass gasifiers demand regular cleaning to remove tar buildup, as well as periodic inspections of feeding mechanisms and combustion chambers to maintain efficiency and avoid downtime. These requirements not only increase operational costs but also necessitate skilled labor and consistent supply chains for biomass feedstock. Similarly, hydrogen tanks require meticulous pressure monitoring and periodic testing to ensure safe operation and compliance with safety standards. The long-term implications of these maintenance needs include higher operational expenditures (OPEX) and potential disruptions in energy supply if maintenance schedules are not rigorously followed. However, advancements in gasifier design, automation of maintenance tasks, and improved hydrogen storage technologies could mitigate these challenges. Therefore, future research should focus on enhancing the durability and automation of these components to minimize operational challenges while maximizing system reliability and economic feasibility.

Figure 10 illustrates the monthly energy production from various sources, including the grid, FCs, solar panels, and BGs. The chart demonstrates a seasonal variation in energy production, with solar panels contributing significantly more energy during the summer months (June to August) than during the winter months (December to February). This variation is expected due to longer daylight hours and higher solar irradiance during summer. During the peak summer months, solar panel contributions reach their maximum, substantially reducing the dependency on grid energy and BGs. Conversely, during winter, energy production from solar panels decreases, leading to increased reliance on grid energy sources and BGs to meet energy demand. Notably, the energy contribution from the BG remained relatively constant throughout the year, providing a stable energy source. The FC contribution remained minimal but consistent across all months, indicating its role as a supplementary energy source rather than a primary source. The grid's energy input increases during winter, compensating for the reduced availability of solar energy. Overall, Fig. 10 highlights the effectiveness of a hybrid energy system in balancing seasonal variations in renewable energy production, thus ensuring a reliable energy supply throughout the year. This demonstrates the strategic advantage of integrating multiple energy sources to enhance the resilience and sustainability of energy systems.

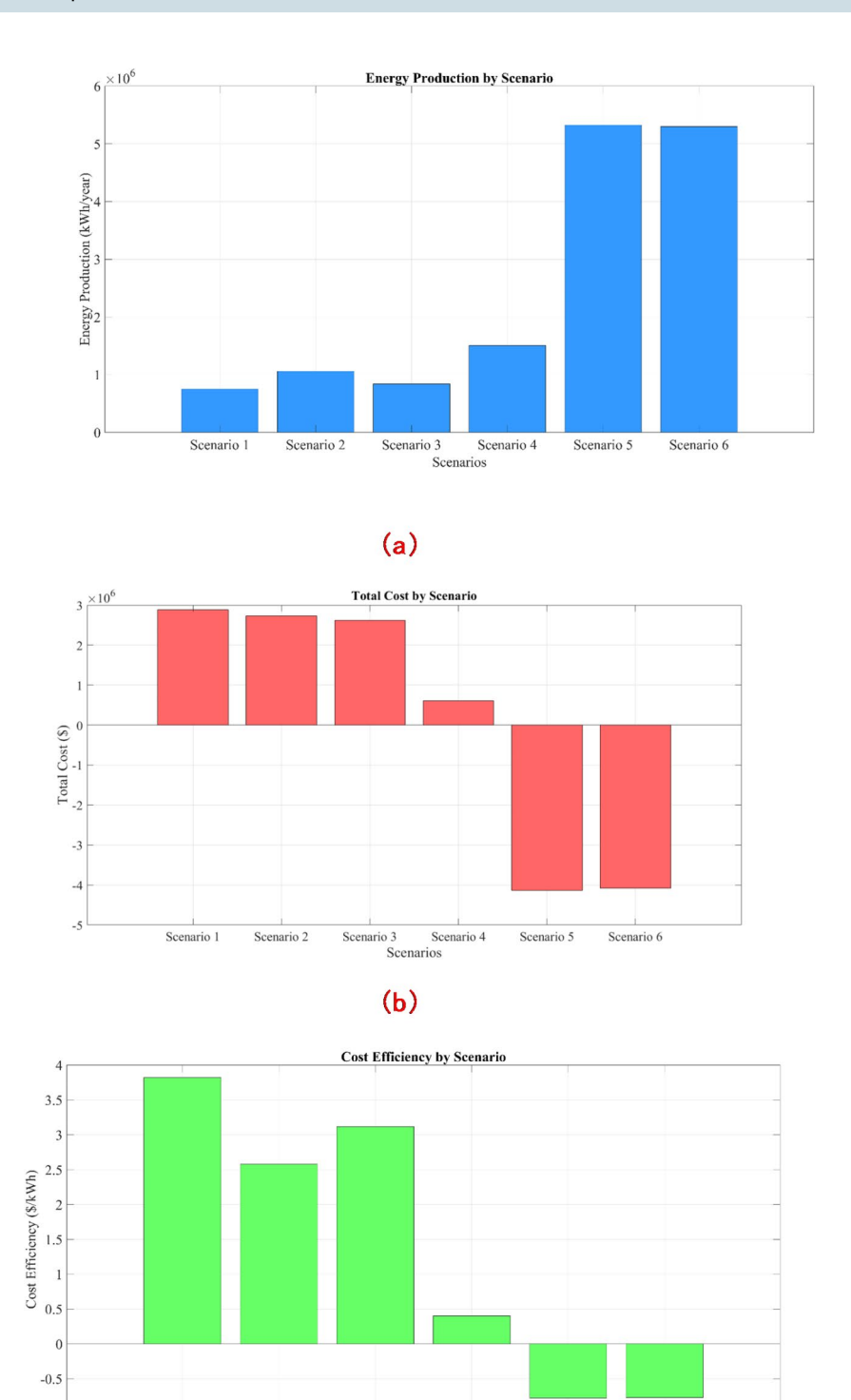


Fig. 9. Comparison of energy production, total costs, and cost efficiency across scenarios.

Scenario 4

Scenario 3

(c)

Scenario 1

Scenario 2

Figure 11 illustrates the daily and hourly energy production of Scenario 4 solar panels throughout the year. The data indicate that from October to February, peak energy production occurs between 09:00 and 14:00 a.m. Conversely, from March to September, the maximum energy production shifted to between 07:00 and 17:00. This variation aligns with the changing daylight hours across seasons, with longer days in summer facilitating extended periods of solar energy production. Annually, the PV system operates for a total of 3,389 h and generates 1,193,484 kWh of energy. The LCOE for the energy produced by the PV panels was calculated to be \$0.0466 per kWh, highlighting the cost-effectiveness of the solar energy component in the hybrid system.

Scenario 5

Scenario 6

Scenario	System components	CAPEX(\$)	OPEX (\$)	Payback period	NPC (\$)	LCOE (\$/kWh)	REF (%)
Scenario 1	PV-BG-HT-Elz-FC-Bat-Inv	1.51 M	65.753	5.66	2.88 M	0.345	100
Scenario 2	PV-WT-Bat-Inv	1.66 M	53.086	6.02	2.73 M	0.327	100
Scenario 3	PV-WT-HT-Elz-FC-Bat-Inv	1.58 M	51.282	5.68	2.62 M	0.313	100
Scenario 4	PV-BG-HT-Elz-FC-Inv-Grid	1.13 M	-25.85	5.98	611,284	0.0215	81.3
Scenario 5	PV-WT-Inv-Grid	6.10 M	- 507.1	8.49	- 4.14 M	- 0.0392	100
Scenario 6	PV-WT-HT-Elz-FC-Bat-Inv-Grid	6.14 M	- 505.5	8.49	- 4.08 M	- 0.0390	98.3

Table 5. Cost and energy production metrics for scenarios one to 6.

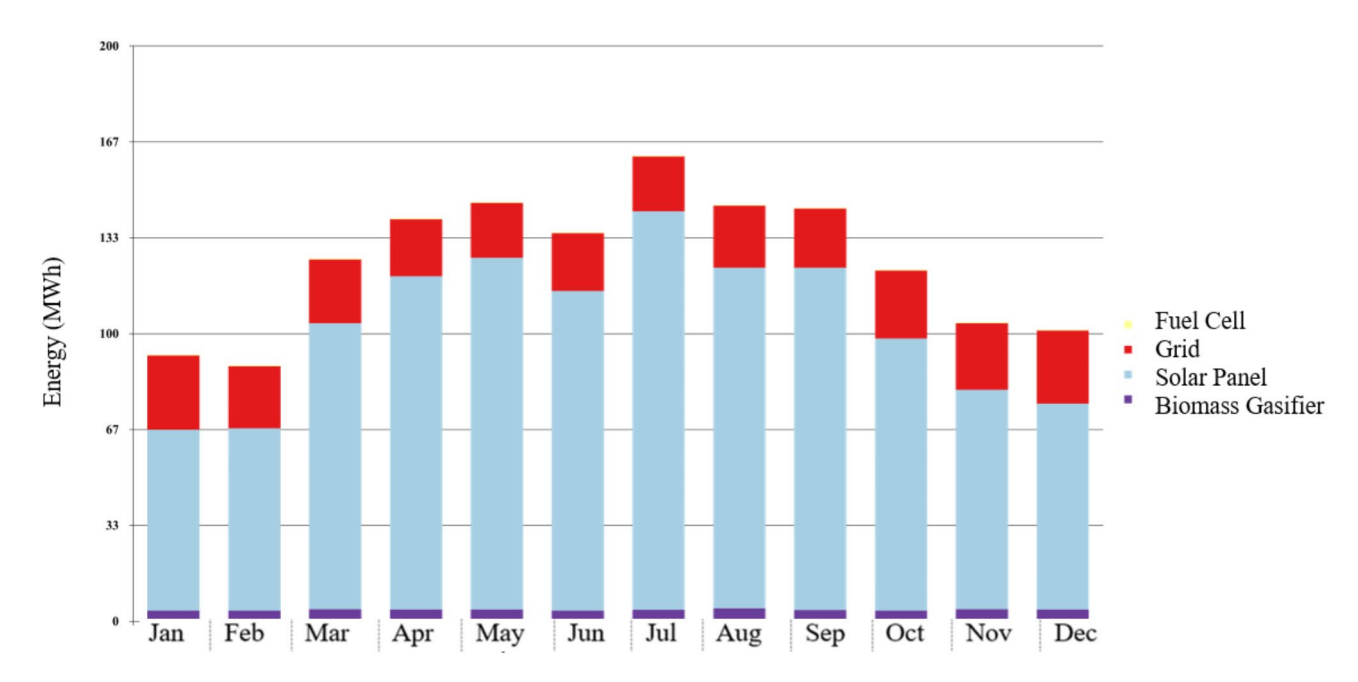


Fig. 10. Monthly energy production of Scenario 4 system components.

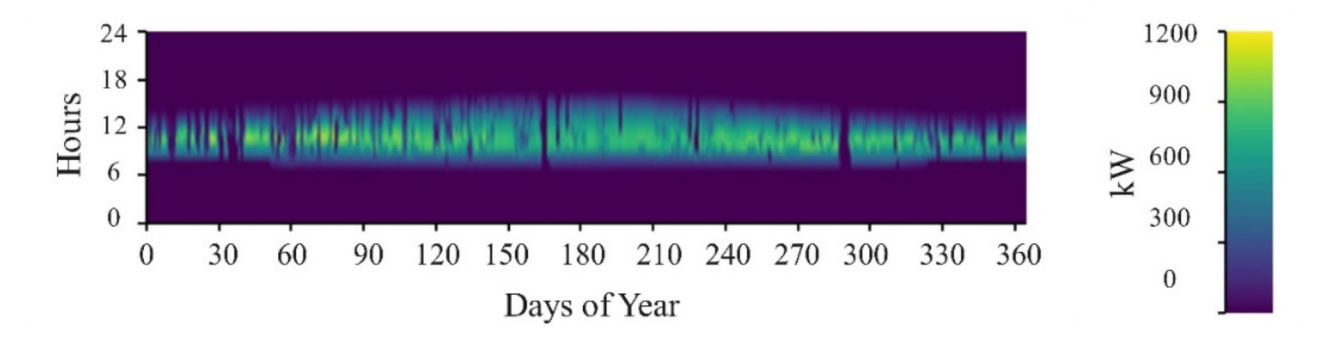


Fig. 11. Daily and hourly energy production for Scenario 4 solar panels.

Strategic use of BGs and grid energy supplements the PV system during periods of low solar irradiance, ensuring consistent and reliable energy supply throughout the year. This comprehensive approach to energy production, as depicted in Fig. 11, underscores the efficacy of Scenario 4's hybrid system in optimizing renewable energy utilization while maintaining economic feasibility. The integration of multiple energy sources in the Çukurova region, which is known for its high solar irradiance, demonstrates a robust model for sustainable and cost-effective energy production.

Figure 12 illustrates the daily and hourly energy production of BG in Scenario 4. The graph shows that the BG primarily operates during the hours of 14:00–20:00, particularly from November to February. This operational pattern aligns with the reduced energy production from the PV system during these hours and months,

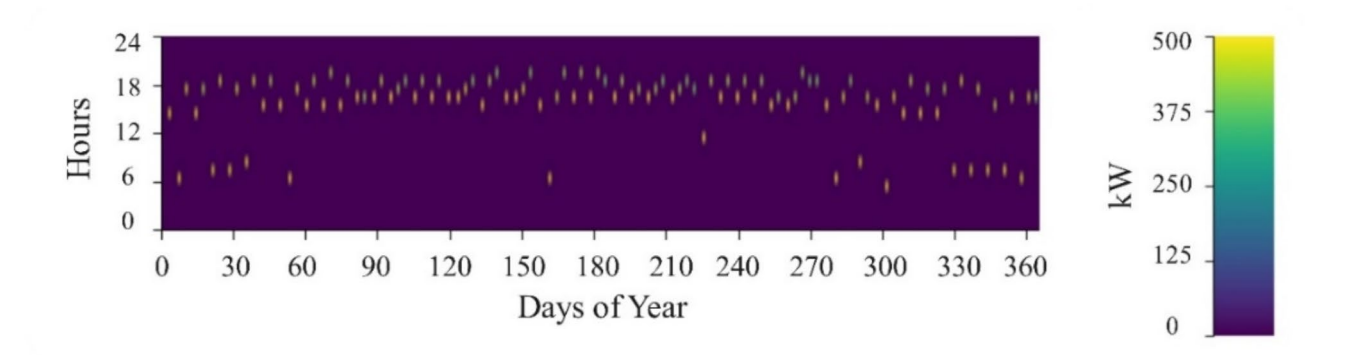


Fig. 12. Daily and hourly energy production of Scenario 4 biomass gasifier.

highlighting the gasifier's role in supplementing energy production when solar output is insufficient. The annual operational time of BG is 105 h, demonstrating its function as a crucial backup energy source during periods of low solar irradiance. The strategic use of the BG ensures a consistent energy supply, compensating for the variability in solar energy production and enhancing the overall reliability of the hybrid system. This integration of the BG, as depicted in Fig. 12, underscores the importance of diverse energy sources for maintaining a stable energy output throughout the year. By effectively balancing the intermittent nature of solar energy with the dependable output from the BG, Scenario 4 achieves a robust and sustainable energy production model.

Figure 13 provides a comprehensive overview of the hydrogen production, storage, and consumption dynamics in Scenario 4. As depicted in Fig. 13a, the electrolyzer's energy production was most active during the daytime hours, particularly in the first half of the year, reflecting the high solar irradiance and extended daylight periods typical of the Çukurova region. Consistent hydrogen production is crucial for maintaining hydrogen supply. Figure 13b shows the hydrogen storage levels in the tank, which remained relatively stable and high throughout the year. This stability is essential for ensuring that hydrogen is readily available to meet energy demands during periods of low renewable energy production. Figure 13c illustrates the hydrogen consumption, which occurs continuously but at a relatively low and stable rate, ensuring balanced usage of the stored hydrogen. This consistent consumption pattern underscores the efficiency of Scenario 4's hybrid system in using hydrogen as a supplementary energy source, thereby enhancing the overall resilience and sustainability of the energy supply. As shown in Fig. 13c, the consumption of 200 kg of hydrogen gas in the HT leads to the production of electrical energy in the FC for 8,353 h annually, except during 09:00 and 13:00. These figures collectively highlight the strategic integration of hydrogen production, storage, and consumption in Scenario 4, demonstrating the viability and efficiency of hydrogen production for maintaining a reliable and sustainable energy system.

Scenario 4 lacks both WT and Bats. The absence of these components is due to the region's low wind speeds, which would increase the system's costs if WTs were included. The inclusion of Bat will lead to significant energy losses and substantially increase system costs. As a result, HOMER Pro microgrid analysis tool version 3.14.2 can identify the most suitable system components. Among the six scenarios, Scenario 4 is the most optimal, producing the highest amount of energy from solar panels, totaling 1,193,484 kWh annually. This scenario is also the most efficient solar electricity generation scenario compared with the other scenarios. During nighttime and winter months, when solar energy is insufficient, biomass and hydrogen are essential. The agricultural suitability of the Adana region enables the BG to produce 48,294 kWh annually, maintaining production during periods of low solar radiation. Another scenario featuring a BG, Scenario 1, produces 46,250 kWh/year from biomass. However, due to Scenario 1's lower PV production of 705,036 kWh/year, the BG's output is insufficient, leading to a higher LCOE. Additionally, Scenario 1's reliance on 13 Bats increases storage costs and NPC. Although hydrogen energy is less commonly preferred due to storage issues, it plays a vital role in Scenario 4. When solar and biomass energy are insufficient, hydrogen FC produces 3,341 kWh annually, reducing the amount of energy purchased from the grid. Other scenarios, such as Scenarios 1, 3, 4, and 6, also use hydrogen technology. Scenario 6 produces 3,344 kWh/year from hydrogen, a figure similar to that of Scenario 4. However, Scenario 6's inclusion of nine Bats raises NPC to \$4,078,430.00. Despite being grid-connected and lacking WTs, Scenario 6's LCOE remains competitive, second only to Scenario 4. The grid connection in Scenario 4 allows the sale of excess energy without the need for BTS, thus reducing costs. As shown in Table 6, Scenario 4 produces 1,507,169 kWh/ year and consumes 1,420,714 kWh/year, indicating that the hybrid system efficiently uses nearly all the energy it generates. This balance ensures a stable energy supply for EVCSs and prevents the energy losses associated with battery storage. Therefore, Scenario 4's design not only optimizes production and consumption but also maintains economic feasibility, making it the most sustainable and cost-effective choice among the scenarios.

Table 7 presents the GHG emissions in Scenarios 1–6. Upon examining the emission rates of air pollutants, Scenario 2 is clearly the most environmentally friendly scenario, while Scenario 4 is the least favorable in terms of emissions. Scenarios 2 and 5, which do not use hydrogen or biomass energy, do not emit CO, unburned hydrocarbons (UHC), particulate matter (PM), SO₂, or NOx gases. Scenario 5, which is a grid-connected system, only contributes to CO₂ emissions. Scenario 2 has the lowest pollutant emissions, with an NPC of \$2,732,353.00 and an LCOE of \$0.327; however, it is not considered a viable system due to its high costs.

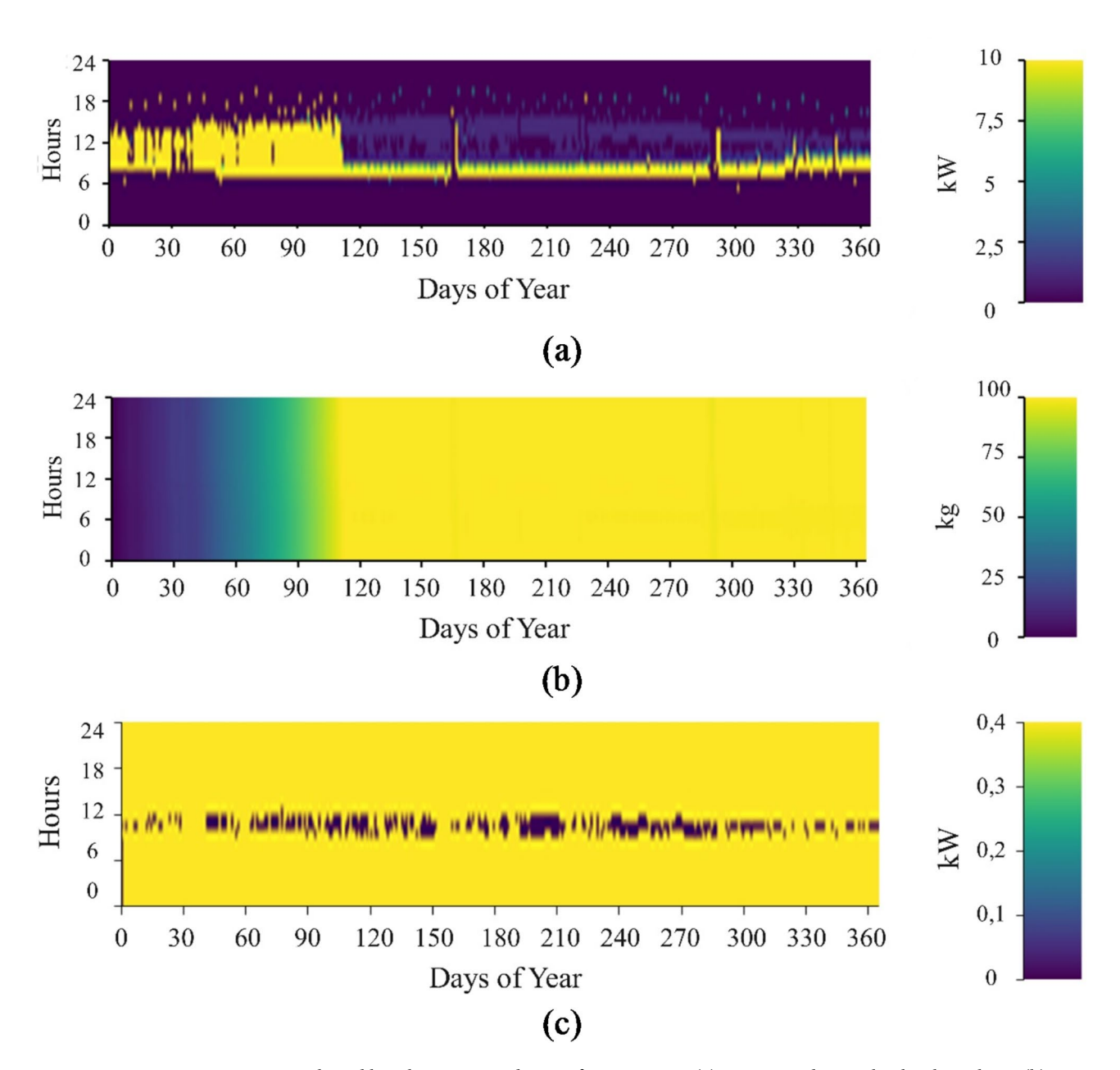


Fig. 13. Daily and hourly energy production for Scenario 4: (a) energy production by the electrolyzer, (b) hydrogen storage in the tank, and (c) hydrogen consumption.

Components	Production (kWh/year)
Solar panel	1,193,484
Fuel cell	3,341
Biomass gasifier	48,294
Grid (purchased energy)	262.05
Total production	1,507,169
	Consumption (kWh/
	year)
AC primary load	
AC primary load Grid (sold energy)	year)

Table 6. Scenario 4: energy production and consumption.

Scenario	Carbon dioxide (kg/year)	Carbon monoxide (kg/year)	Unburned hydrocarbons (kg/year)	Particulate matter (kg/year)	Sulfur dioxide (kg/year)	Nitrogen oxide levels (kg/year)
Scenario 1	24,80	1,16	0.0960	0.0654	0	7,92
Scenario 2	0	-	-	-	-	-
Scenario 3	- 1.65	1.05	0.117	0.0793	0	9,39
Scenario 4	165,67	1.59	0.144	0.0983	718	363
Scenario 5	74,83	-	-	-	-	-
Scenario 6	55,78	1.30	0.144	0.0983	242	130

Table 7. Scenario 1-2-3-4-5-6 greenhouse emissions.

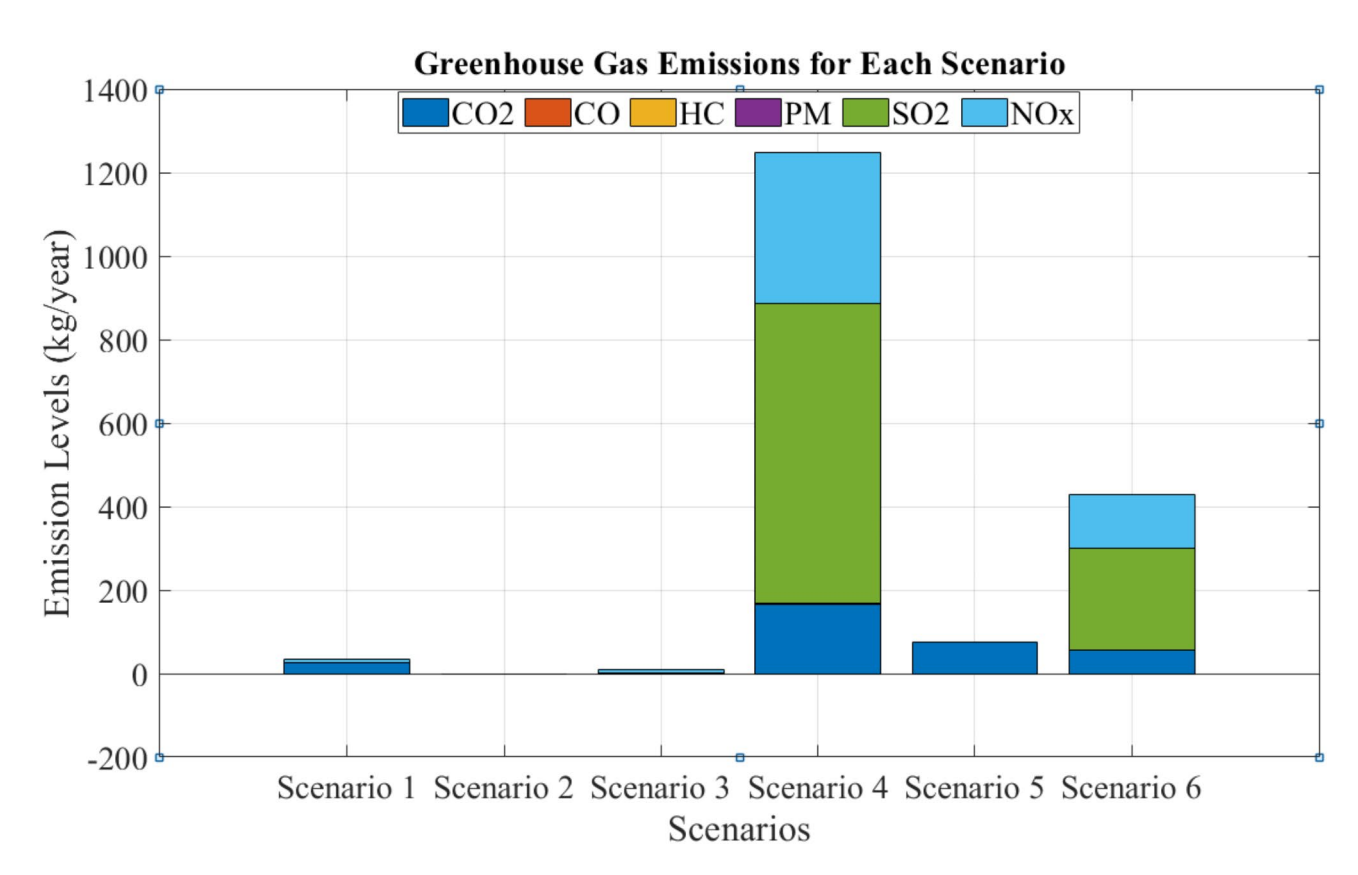


Fig. 14. Greenhouse gas emissions for each scenario.

In contrast, Scenario 4, which exhibits the highest pollutant emissions, is deemed the most viable system due to its optimal NPC and LCOE values. Although Scenario 4 generates significant emissions of CO₂, CO, UHC, PM, SO₂, and NOx, its economic feasibility overshadows these environmental concerns. In systems using fossil fuels, the type of fossil fuel used dictates the extent of GHG emission, which is generally much higher than that in systems incorporating renewable energy sources. Therefore, despite its higher emissions, Scenario 4's pollutants are relatively minor when juxtaposed with traditional fossil fuel systems. Thus, Scenario 4 emerges as the most practical option, with its pollutant emissions deemed acceptable given its significant economic and sustainability benefits.

As depicted in Fig. 14, the inclusion of biomass in Scenario 4 results in higher emissions of NOx and SO₂ compared to PV and WT-only systems. Nevertheless, leveraging agricultural waste as a biomass source ensures a closed carbon cycle, which helps to offset these emissions and reduces the net environmental impact. Hydrogen integration further enhances the system's potential to lower carbon emissions, particularly when derived from renewable energy. Although Scenario 4 demonstrates elevated GHG emissions relative to other renewable-focused scenarios, its emissions remain significantly lower than those of conventional fossil fuel-based systems. This underscores the balance between economic feasibility and environmental considerations in hybrid configurations. Advanced hydrogen production methods and carbon capture technologies could further minimize emissions, ensuring long-term sustainability.

Figure 15 shows the percentage of renewable energy output for Scenario 4, highlighting that between the hours of 06:00 and 18:00, during peak traffic times in the morning and evening, energy is predominantly produced from clean energy sources. During these hours, no energy is purchased from the grid, indicating

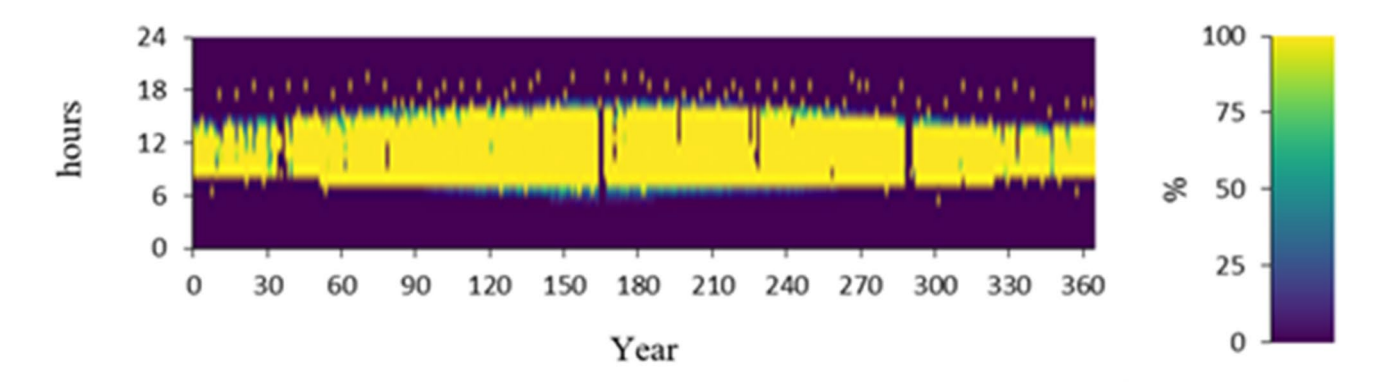


Fig. 15. Percentage of renewable energy (REF) for Scenario 4.

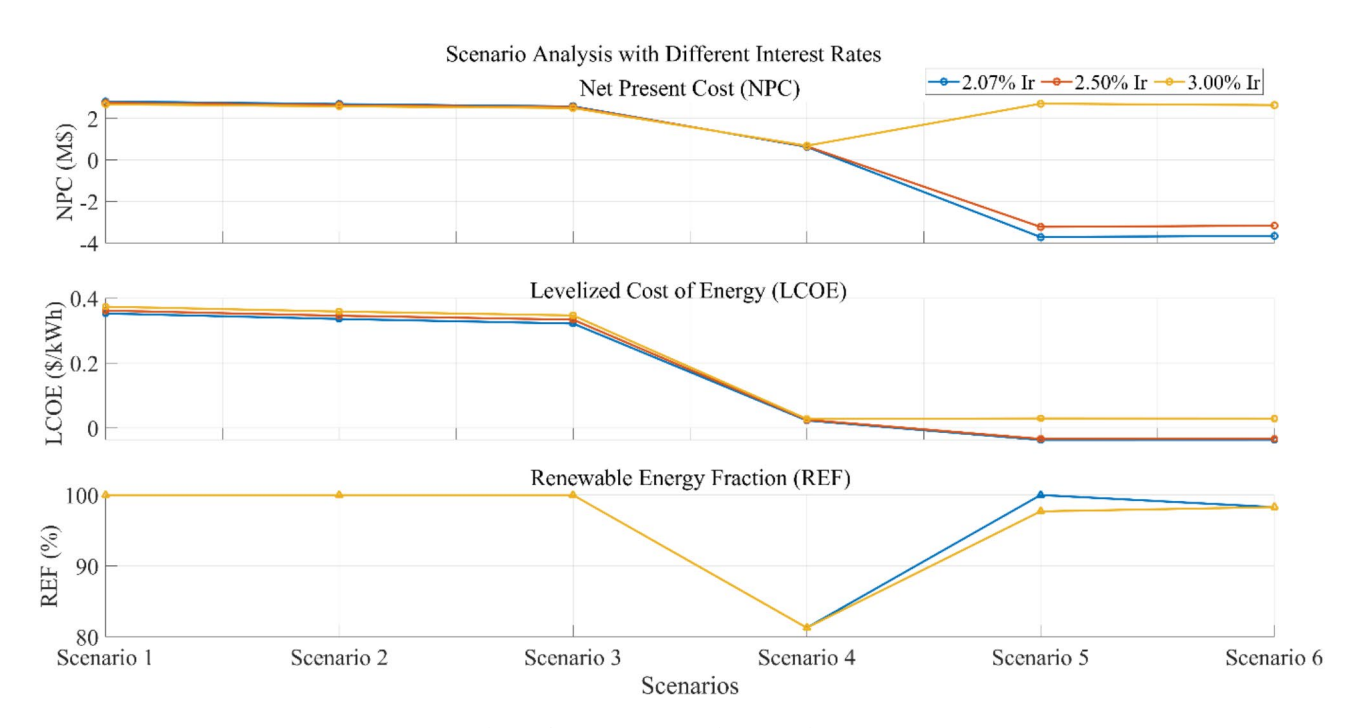


Fig. 16. Sensitivity analysis of NPC, LCOE, and REF under varying interest rates.

the system's efficiency in meeting the demand for renewable energy. This suggests that if the current fossil fuel-based energy systems used to power EVCSs are replaced with hybrid systems incorporating renewable energy sources, there will be a substantial reduction in carbon emissions. Consistent use of renewable energy during high-demand periods demonstrates the potential for significant environmental benefits through the adoption of hybrid systems.

Sensitivity analysis of HRES

Sensitivity analysis serves as a critical tool for evaluating the performance of a system by examining the effects of variations in key parameters on system optimization. In this study, two primary parameters were analyzed: the annual discount rate and the load demand level. By systematically varying these parameters and assessing the resulting changes in system optimization outcomes, valuable insights were gained regarding the robustness and adaptability of the proposed scenarios. This approach not only highlights the critical influence of these parameters but also provides a deeper understanding of the operational flexibility and economic feasibility of HRESs under varying conditions.

Impact of real interest (i_r)

The sensitivity analysis results, illustrated in Fig. 16, demonstrate the impact of varying interest rates (2.07%, 2.50%, and 3.00%) on the NPC, LCOE, and REF across the six scenarios. As shown, Scenario 4 consistently achieves the lowest NPC and LCOE under all interest rate conditions, highlighting its economic feasibility. Furthermore, Scenario 4 maintains a high REF, ensuring significant reliance on renewable energy sources while minimizing grid dependency. In contrast, Scenarios 5 and 6, despite their higher renewable fractions, exhibit

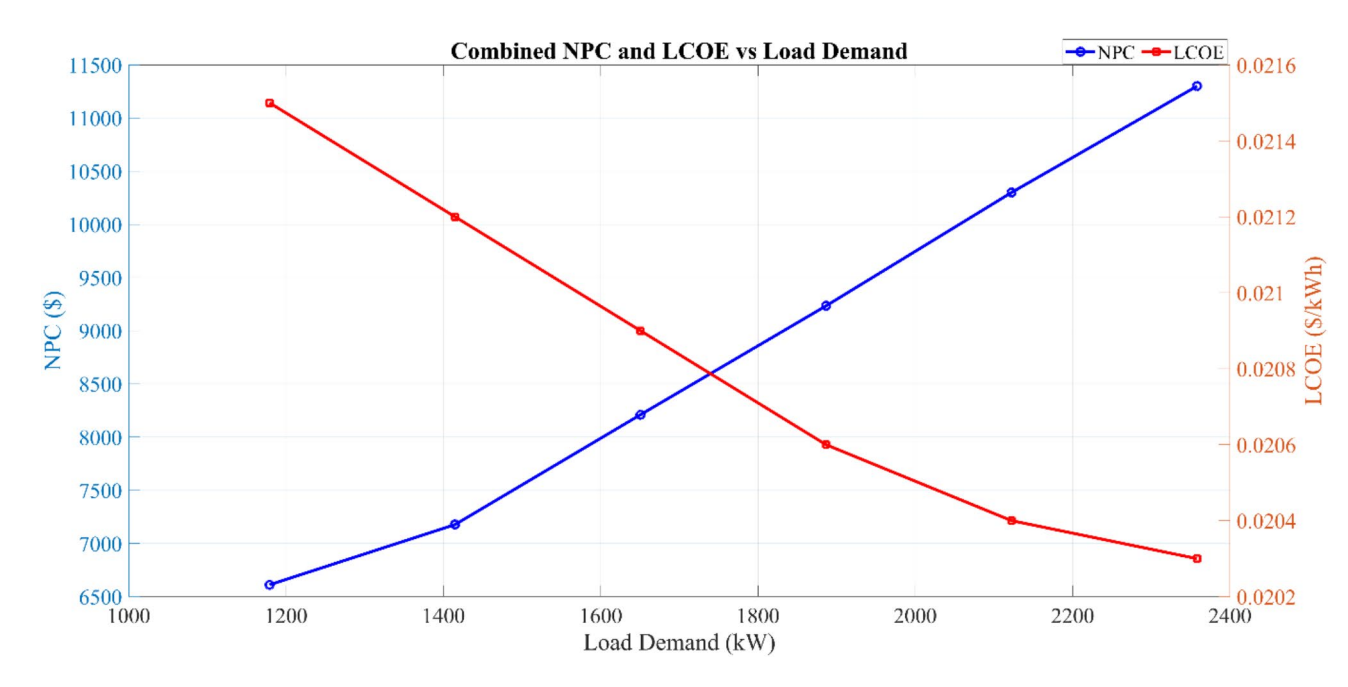


Fig. 17. Sensitivity analysis of NPC, LCOE, and REF under varying interest rates.

Variations in load	Nominal load	20% Increase	40% Increase	60% Increase	80% Increase	100% Increase
Load demand (kW)	1179	1414.80	1650.60	1886,40	2122.20	2358
NPC (\$)	6611,284	717,372	821.141	923.397	1.03 M	1.13 M
LCOE (\$/kWh)	0.0215	0.0212	0.0209	0.0206	0.0204	0.0203

Table 8. Impact of load fluctuations on HRES sizing and cost.

negative NPC values and infeasible LCOE results due to excessive reliance on external grid connections. These findings emphasize the robustness of Scenario 4 under varying economic conditions, making it the most optimal configuration for cost-effective and sustainable EVCS operations.

Impact of load variations

As illustrated in Fig. 17 and detailed in Table 8, the HRES exhibits a significant increase in NPC as load demand rises from its nominal value of 1179 kW to 2358 kW, with NPC escalating from \$611,284 to \$1.13 M. Conversely, the LCOE demonstrates a marginal decline over the same range, decreasing from \$0.0215/kWh to \$0.0203/kWh. This inverse relationship between NPC and LCOE highlights the system's scalability and cost optimization potential. The results suggest that while the system incurs higher upfront costs to accommodate increased load, its energy production becomes more cost-effective on a per-unit basis. These findings underscore the robustness and economic viability of the proposed HRES design in addressing dynamic load requirements.

Conclusions

The increasing GHG emissions, which contribute to rising temperatures and climate change, have heightened the demand for RESs. This shift has also accelerated the transition to EVs in the transportation sector. Consequently, ensuring a reliable and continuous electricity supply for EVCSs has become crucial, emphasizing the importance of hybrid systems that integrate RESs. Various software tools and programs have been developed to address these challenges.

This study investigates the most suitable hybrid systems for providing electricity to EVCSs in the Çukurova region of Adana. Six different scenarios consisting of combinations of the PV, WT, BG, Elz, HT, FC, Bat, Inv, and Grid components were evaluated. The simulations were conducted using HOMER Pro microgrid analysis tool version 3.14.2 software developed by NREL, with each scenario's energy production and consumption results analyzed in detail. The optimization results indicate that Scenario 4, comprising PV, BG, Elz, HT, FC, Inv, and Grid, is the most feasible system. Scenario 4 has an NPC of \$611,283.50 and an LCOE of \$0.0215. The annual energy production and consumption were 1,507,169 kWh and 1,420,714 kWh, respectively. The analysis demonstrates that the region's PV efficiency significantly benefits the overall system. In addition, the inclusion of biomass and hydrogen energy systems ensures continuous production during periods of insufficient solar energy. However, due to the region's low average wind speeds, the contribution of WT to the system is limited and is not included among the components of Scenario 4. The annual energy purchased from the grid was 262.05 kWh, while the energy sold to the grid was 976,447 kWh. This surplus of energy generated from RES

over that purchased from the grid shortens the system's payback period, enhancing its economic viability. The significant impact of solar energy on the performance and cost-effectiveness of EVCS underscores its potential as an advantageous option.

These findings underscore the growing necessity of integrating renewable energy systems into EVCS infrastructure, particularly in regions like Turkey, where the rapid increase in EVs poses significant challenges for the national grid. The dependency of EVCS on grid-based electricity is expected to strain the grid further, potentially leading to energy imbalances and increased operational costs. This study emphasizes the importance of meeting EVCS energy demands through renewable and hybrid systems, reducing the burden on the grid while enhancing energy sustainability. By aligning with Turkey's renewable energy potential, this approach not only mitigates the risks of grid dependency but also contributes to the development of a resilient and efficient energy framework for the expanding EVCS network.

To facilitate the implementation of such systems, policy measures such as subsidies for renewable energy infrastructure, feed-in tariffs for surplus energy, and long-term tax exemptions for HRES installations could play a crucial role. Additionally, green financing schemes could reduce upfront capital costs, making these systems more accessible. Future research should focus on addressing areas beyond this study's scope. While hydrogen-based technologies such as fuel cells and electrolyzers were analyzed, exploring hybrid configurations with combined hydrogen and BTS could optimize flexibility and costs. Advanced turbine designs or offshore wind resources may overcome the limitations of low wind speeds observed in regions like Çukurova. Expanding these systems to diverse climatic and demand profiles, coupled with strong policy frameworks and economic incentives, would further refine their feasibility. Additionally, evaluating the environmental impact of HRES components through life cycle assessments is essential for ensuring sustainability and long-term viability.

Data availability

The datasets used and/or analysed during the current study available from the corresponding author on reasonable request.

Received: 1 October 2024; Accepted: 23 January 2025

Published online: 04 February 2025

References

- 1. Ahmad, F., Khalid, M. & Panigrahi, B. K. An enhanced approach to optimally place the solar powered electric vehicle charging station in distribution network. *J. Energy Storage* 42, 103090 (2021).
- Alhousni, F. K. et al. Photovoltaic power prediction using analytical models and homer-pro: investigation of results reliability. Sustain 15, 89 (2023).
- 3. Zhou, G., Zhu, Z. & Luo, S. Location optimization of electric vehicle charging stations: based on cost model and genetic algorithm. *Energy* **247**, 123437 (2022).
- 4. Zhang, M. et al. Optimized control of hybrid energy storage systems for microgrids. J. Phys. Conf. Ser. 2846, 012033 (2024).
- 5. Eid, A., Mohammed, O. & El-Kishky, H. Efficient operation of battery energy storage systems, electric-vehicle charging stations and renewable energy sources linked to distribution systems. *J. Energy Storage* 55, 105644 (2022).
- Abid, M. S., Ahshan, R., Al Abri, R., Al-Badi, A. & Albadi, M. Techno-economic and environmental assessment of renewable energy sources, virtual synchronous generators, and electric vehicle charging stations in microgrids. *Appl. Energy.* 353, 122028 (2024).
- Sierra, A., Gercek, C., Geurs, K. & Reinders, A. Technical, financial, and environmental feasibility analysis of photovoltaic EV charging stations with energy storage in China and the United States. IEEE J. Photovoltaics. 10, 1892–1899 (2020).
- Rajeevkumar Urs, R., Mussawar, O., Zaiter, I., Mezher, T. & Mayyas, A. Navigating the cost-efficiency Frontier: exploring the viability of Grid-connected energy storage systems in meeting district load demand. *Energy Convers. Manag.* 299, 117828 (2024).
- 9. Karmaker, A. K., Prakash, K., Siddique, M. N. I., Hossain, M. A. & Pota, H. Electric vehicle hosting capacity analysis: challenges and solutions. *Renew. Sustain. Energy Rev.* 189, 113916 (2024).
- Pareek, S., Sujil, A., Ratra, S. & Kumar, R. Electric vehicle charging station challenges and opportunities: a future perspective. In Proc—2020 Int. Conf. Emerg. Trends Commun. Control Comput. ICONC3 2020 1–5 (2020).
- 11. Nasir, T. et al. Optimal scheduling of campus microgrid considering the electric vehicle integration in smart grid. Sensors 21, 1–20 (2021).
- 12. Roslan, M. F. et al. Techno-economic impact analysis for renewable energy-based hydrogen storage integrated grid electric vehicle charging stations in different potential locations of Malaysia. *Energy Strateg Rev.* 54, 101478 (2024).
- Zhao, Z., Lee, C. K. M. & Ren, J. A two-level charging scheduling method for public electric vehicle charging stations considering heterogeneous demand and nonlinear charging profile. Appl. Energy 355, 122278 (2024).
- Kumar, M., Shaikh, M. A., Soomro, A. M., Kazmi, A., Kumar, A. & S. A. & Techno-economic comparative analysis of an offgrid PV-wind-hydrogen based EV charging station under four climatically distinct cities in Pakistan. *Int. J. Hydrogen Energy* 93, 1268–1282 (2024).
- 15. Irham, A. et al. Cost-effectiveness and reliability evaluation of hydrogen storage-based hybrid energy systems for unreliable grid. *Int. J. Hydrogen Energy* **94**, 1314–1328 (2024).
- Zhang, M., Yan, Q., Guan, Y. & Ni, D. & Agundis Tinajero, G. D. Joint planning of residential electric vehicle charging station integrated with photovoltaic and energy storage considering demand response and uncertainties. *Energy* 298, 859 (2024).
- 17. Li, H., Son, D. & Jeong, B. Electric vehicle charging scheduling with mobile charging stations. J. Clean. Prod. 434, 140162 (2024).
- 18. Nareshkumar, K. & Das, D. Optimal location and sizing of electric vehicles charging stations and renewable sources in a coupled transportation-power distribution network. *Renew. Sustain. Energy Rev.* 203, 114767 (2024).
- 19. Soomro, A. M. et al. Techno-economic analysis of stand-alone hybrid PV-hydrogen-based plug-in electric vehicle charging station. *Energy Rep.* 12, 3279–3290 (2024).
- 20. Modu, B., Abdullah, M. P., Alkassem, A. & Hamza, M. F. Optimal rule-based energy management and sizing of a grid-connected renewable energy microgrid with hybrid storage using Levy Flight Algorithm. *Energy Nexus* 16, 100333 (2024).
- Ahmad, F. & Bilal, M. Allocation of plug-in electric vehicle charging station with integrated solar powered distributed generation using an adaptive particle swarm optimization. *Electr. Eng.* 106, 2595–2608 (2024).
 Abdel-Basset, M., Gamal, A., Hezam, I. M. & Sallam, K. M. Sustainability assessment of optimal location of electric vehicle
- Abdel-Basset, M., Gamal, A., Hezam, I. M. & Sallam, K. M. Sustainability assessment of optimal location of electric vehicle charge stations: a conceptual framework for green energy into smart cities. In *Environment, Development and Sustainability vol. 2* (Springer Netherlands, 2024).

- Kumar, B. A. et al. Hybrid genetic algorithm-simulated annealing based electric vehicle charging station placement for optimizing distribution network resilience. Sci. Rep. 14, 7637 (2024).
- 24. Yao, M., Da, D., Lu, X. & Wang, Y. A. A review of capacity allocation and control strategies for electric vehicle charging stations with integrated photovoltaic and energy storage systems. World Electr. Veh. J. 15, 785 (2024).
- 25. Karmaker, A. K., Hossain, M. A., Pota, H. R., Onen, A. & Jung, J. Energy management system for hybrid renewable energy-based electric vehicle charging station. *IEEE Access* 11, 27793–27805 (2023).
- Oladigbolu, J. O., Mujeeb, A., Al-Turki, Y. A. & Rushdi, A. M. A novel doubly-green stand-alone electric vehicle charging station in Saudi Arabia: an overview and a comprehensive feasibility study. *IEEE Access* 11, 37283–37312 (2023).
- 27. Priyanka, T. J., Atre, S., Billal, M. M. & Arani, M. Techno-economic analysis of a renewable-based hybrid energy system for utility and transportation facilities in a remote community of Northern Alberta. Clean. Energy Syst. 6, 748 (2023).
- 28. Direya, R. & Khatib, T. Simplified python models for photovoltaic-based charging stations for electric vehicles considering technical, economic, and environmental aspects. World Electr. Veh. J. 14, 145 (2023).
- 29. Ourya, I., Nabil, N., Abderafi, S., Boutammachte, N. & Rachidi, S. Assessment of green hydrogen production in Morocco, using hybrid renewable sources (PV and wind). *Int. J. Hydrogen Energy* 48, 37428–37442 (2023).
- Singh, R., Gupta, A., Singh, D. & Paul, A. R. Design and assessment of an electric vehicle charging station using hybrid renewable energy. *Int. J. Energy Clean. Environ.* 23, 31–47 (2022).
- 31. Muna, Y. B. & Kuo, C. C. Feasibility and techno-economic analysis of electric vehicle charging of PV/wind/diesel/battery hybrid energy system with different battery technology. *Energies* 2022, 15 (2022).
- 32. Isik, U. M., Tercan, S. M. & Gokalp, E. Optimal sizing and detailed analysis of microgrid with photovoltaic panel and battery energy storage system integrated electric vehicle charging station. In HORA 2023—2023 5th Int. Congr. Human-Computer Interact. Optim. Robot. Appl. Proc. (2023).
- 33. Jaganath, M. M., Ray, S. & Choudhury, N. B. D. Eco-friendly microgrid carport charging station for electric vehicles (EVs). e-Prime Adv. Electr. Eng. Electron. Energy. 5, 100196 (2023).
- Patil, R. D., Veena, S. & Sridhar, H. Design and evaluation of charging stations including renewables and storage. In 2019 Glob. Conf. Adv. Technol. GCAT 2019 20–25 (2019).
- 35. Ganie, N. A., Rather, Z. H., Farooq, Z. & Rahman, A. Economic feasibility of SPV integrated EV charging infrastructure for NIT Srinagar institutional campus in J&K, India. In 2023 Int. Conf. Power, Instrumentation, Energy Control. PIECON 2023 1–6 (2023).
- 36. Adefarati, T., Obikoya, G. D., Sharma, G., Onaolapo, A. K. & Akindeji, K. T. Design and Feasibility Analysis of Grid-Connected Hybrid Renewable Energy System: Perspective of Commercial Buildings. Energy systems, vol. 15 (Springer, 2024).
- 37. Zhang, Y. et al. HOMER-based multi-scenario collaborative planning for grid-connected PV-storage microgrids with electric vehicles. *Processes* 11, 2408 (2023).
- 38. Bimenyimana, S. et al. IIntegration of microgrids and electric vehicle technologies in the national grid as the key enabler to the sustainable development for Rwanda. *Int. J. Photoenergy* **2021**, 1–17 (2021).
- 39. Ullah, Z. et al. Optimal scheduling and techno-economic analysis of electric vehicles by implementing solar-based grid-tied charging station. *Energy* **267**, 126560 (2023).
- 40. Rehman, S., Mohammed, A. B., Alhems, L. & Alsulaiman, F. Comparative study of regular and smart grids with PV for electrification of an academic campus with EV charging. *Environ. Sci. Pollut Res.* 30, 77593–77604 (2023).
- 41. Parida, B. K. & Kumar Bohre, A. Optimal sizing of PV, wind based grid connected hybrid renewable energy systems for rural areas in presence of EVs. In 2022 Int. Conf. Decis. Aid Sci. Appl. DASA 2022 1311–1316 (2022).
- 42. Terkes, M., Tercan, S. M., Demirci, A. & Gokalp, E. An evaluation of renewable fraction using energy storage for electric vehicle charging station. In 2022 International Congress on Human-Computer Interaction, Optimization and Robotic Applications (HORA) 1–10 (IEEE, 2022).
- 43. Sood, S., Kumar, R. & Tiwari, N. K. Enviro-economic assessment of energy sources used for electric vehicle charging. In 2022 1st Int. Conf. Sustain. Technol. Power Energy Syst. STPES 2022 1–5 (2022).
- 44. Minh, P. V., Quang, L., Pham, M. H. & S. & Technical economic analysis of photovoltaic-powered electric vehicle charging stations under different solar irradiation conditions in Vietnam. *Sustain* 13, 15–25 (2021).
- Chakraborty, I. & Bohre, A. K. Effect of thermal load on HRES for a rural area using different types of loads and sources. In Proc. 2022 6th Int. Conf. Cond. Assess. Tech. Electr. Syst. CATCON 2022, vol. 5 313–317 (2022).
- 46. Güven, A. F. Heuristic Techniques and Evolutionary Algorithms in Microgrid Optimization Problems (eds. Microgrid) (CRC, 2024).
- 47. Güven, A. F., Yörükeren, N. & Samy, M. M. Design optimization of a stand-alone green energy system of university campus based on Jaya-Harmony Search and ant colony optimization algorithms approaches. *Energy* **253**, 124089 (2022).
- 48. Guven, A. F., Yorukeren, N., Tag-Eldin, E. & Samy, M. M. Multi-objective optimization of an Islanded Green energy system utilizing sophisticated hybrid metaheuristic approach. *IEEE Access.* 11, 103044–103068 (2023).
- 49. See, A. M. K. et al. Techno-economic analysis of an off-grid hybrid system for a remote island in Malaysia: Malawali island, Sabah. Renew. Sustain. Energy Transit. 2, 100040 (2022).
- 50. El-Sattar, H. A., Kamel, S., Sultan, H. M., Zawbaa, H. M. & Jurado, F. Optimal design of photovoltaic, biomass, fuel cell, hydrogen tank units and electrolyzer hybrid system for a remote area in Egypt. *Energy Rep.* 8, 9506–9527 (2022).
- 51. Kashefi Kaviani, A., Riahy, G. H. & Kouhsari, S. M. Optimal design of a reliable hydrogen-based stand-alone wind/PV generating system, considering component outages. *Renew. Energy* 34, 2380–2390 (2009).
- 52. Güven, A. F. & Mahmoud Samy, M. Performance analysis of autonomous green energy system based on multi and hybrid metaheuristic optimization approaches. *Energy Convers. Manag.* **269**, 116058 (2022).
- 53. Vendoti, S., Muralidhar, M. & Kiranmayi, R. Techno-economic analysis of off-grid solar/wind/biogas/biomass/fuel cell/battery system for electrification in a cluster of villages by HOMER software. *Environ. Dev. Sustain.* 23, 351–372 (2021).
- Cano, A., Arévalo, P. & Jurado, F. Energy analysis and techno-economic assessment of a hybrid PV/HKT/BAT system using biomass gasifier: Cuenca-Ecuador case study. *Energy* 202, 117727 (2020).
- 55. Eteiba, M. B., Barakat, S., Samy, M. M. & Wahba, W. I. Optimization of an off-grid PV/Biomass hybrid system with different battery technologies. Sustain. Cities Soc. 40, 713–727 (2018).
- Güven, A. F. & Akbaşak, S. B. Elektrikli araçlarda DA Hızlı Şarj Ünitelerinin Şebeke altyapısına etkilerinin İncelenmesi. Sinop Üniversitesi Fen Bilim Derg. 6, 42–54 (2021).
- 57. Guven, A. F. Integrating electric vehicles into hybrid microgrids: a stochastic approach to future-ready renewable energy solutions and management. *Energy* **303**, 131968 (2024).
- 58. Boddapati, V. & Daniel, S. A. Design and feasibility analysis of hybrid energy-based electric vehicle charging station. *Distrib. Gener Altern. Energy J.* 37, 41–72 (2022).
- 59. Güven, A. F. & Mengi, O. Ö. Assessing metaheuristic algorithms in determining dimensions of hybrid energy systems for isolated rural environments: exploring renewable energy systems with hydrogen storage features. *J. Clean. Prod.* 428, 139339 (2023).
- 60. Boddapati, V., Kumar, R., Arul Daniel, A., Padmanaban, S. & S. & Design and prospective assessment of a hybrid energy-based electric vehicle charging station. *Sustain. Energy Technol. Assess.* 53, 102389 (2022).

Acknowledgements

The authors would like to acknowledge the Deanship of Graduate Studies and Scientific Research, Taif University for funding this work.

Author contributions

Aykut Fatih GÜVEN, Nilya ATEŞ: Conceptualization, Methodology, Software, Visualization, Investigation, Writing- Original draft preparation. Saud ALOTAIBI, Thabet ALZAHRANI, Amare Merfo AMSAL, Salah K. ELSAYED: Data curation, Validation, Supervision, Resources, Writing - Review & Editing, Project administration; Salah K. ELSAYED, Fund acquisition.

Funding

This work is funded and supported by the Deanship of Graduate Studies and Scientific Research, Taif University.

Competing interests

The authors declare no competing interests.

Additional information

Correspondence and requests for materials should be addressed to A.F.G. or A.M.A.

Reprints and permissions information is available at www.nature.com/reprints.

Publisher's note Springer Nature remains neutral with regard to jurisdictional claims in published maps and institutional affiliations.

Open Access This article is licensed under a Creative Commons Attribution-NonCommercial-NoDerivatives 4.0 International License, which permits any non-commercial use, sharing, distribution and reproduction in any medium or format, as long as you give appropriate credit to the original author(s) and the source, provide a link to the Creative Commons licence, and indicate if you modified the licensed material. You do not have permission under this licence to share adapted material derived from this article or parts of it. The images or other third party material in this article are included in the article's Creative Commons licence, unless indicated otherwise in a credit line to the material. If material is not included in the article's Creative Commons licence and your intended use is not permitted by statutory regulation or exceeds the permitted use, you will need to obtain permission directly from the copyright holder. To view a copy of this licence, visit http://creativecommons.org/licenses/by-nc-nd/4.0/.

© The Author(s) 2025